Reducing the two-loop large-scale structure power spectrum to low-dimensional, radial integrals

Marcel Schmittfull[1,4] and Zvonimir Vlah[2,3]

[1]*Berkeley Center for Cosmological Physics, Department of Physics and Lawrence Berkeley National Laboratory, University of California, Berkeley, California 94720, USA*
[2]*Stanford Institute for Theoretical Physics and Department of Physics, Stanford University, Stanford, California 94306, USA*
[3]*Kavli Institute for Particle Astrophysics and Cosmology, SLAC and Stanford University, Menlo Park, California 94025, USA*
[4]*Institute for Advanced Study, Einstein Drive, Princeton, New Jersey 08540, USA*

Modeling the large-scale structure of the universe on nonlinear scales has the potential to substantially increase the science return of upcoming surveys by increasing the number of modes available for model comparisons. One way to achieve this is to model nonlinear scales perturbatively. Unfortunately, this involves high-dimensional loop integrals that are cumbersome to evaluate. Trying to simplify this, we show how two-loop (next-to-next-to-leading order) corrections to the density power spectrum can be reduced to low-dimensional, radial integrals. Many of those can be evaluated with a one-dimensional fast Fourier transform, which is significantly faster than the five-dimensional Monte-Carlo integrals that are needed otherwise. The general idea of this fast fourier transform perturbation theory method is to switch between Fourier and position space to avoid convolutions and integrate over orientations, leaving only radial integrals. This reformulation is independent of the underlying shape of the initial linear density power spectrum and should easily accommodate features such as those from baryonic acoustic oscillations. We also discuss how to account for halo bias and redshift space distortions.

I. INTRODUCTION

Observations of the large-scale structure (LSS) of the universe are becoming increasingly precise and abundant, with many large surveys planned in the near future, including e.g. DES [1], eBOSS [2], DESI [3], Euclid [4], WFIRST [5], LSST [6], and SPHEREx [7]. It is exciting to use this observational window to study fundamental physics and the evolution and composition of the universe. This is possible because properties of the constituents of the universe leave characteristic fingerprints in the observed distribution of LSS, enabling detailed studies of e.g. dark energy, the initial conditions from the big bang, neutrinolike particles, or modifications of general relativity. The accuracy with which we can study these fingerprints is set by the number of independent three-dimensional modes that we can model and include in data analyses. This is in turn determined by the smallest scale that we can still model. Therefore, an important aspect of large-scale structure research is to extend the validity of models to smaller, more nonlinear scales.

Given the immense effort put into future surveys and the strong dependence of their science output on the smallest scale that can be modeled, any idea for improving LSS models on small scales is worth pursuing. This has therefore been an area of intense study in the literature. The two main perturbative modeling approaches are Eulerian standard perturbation theory (SPT) (e.g. [8–12]) and Lagrangian perturbation theory (LPT) (e.g. [13–15]); see [16] for a review and e.g. [17–40] for a selection of more recent developments. Higher-order perturbative corrections to these models push their validity to smaller scales. However these corrections involve high-dimensional, computationally expensive loop integrals. For example, the 2-loop power spectrum in SPT involves five-dimensional integrals at every wave number of interest. Accurate numerical evaluation of the 2-loop power spectrum can therefore take several CPU hours for a single set of cosmological parameter values. Reducing the computational complexity can make these 2-loop integrals more practicable for the LSS community, and simplify their use for constraining cosmological parameters from LSS surveys with Monte-Carlo chains, which often require evaluating model predictions for thousands of cosmological parameter values.

Motivated by this, we recently proposed a fast method to evaluate the 1-loop, next-to-leading-order matter power spectrum from an arbitrary linear input power spectrum [41]. Reference [42] presented the same method for 2-2 contributions and an alternative method for 1-3 couplings. Related work that separates high-dimensional integrals into products of lower dimensional integrals includes [36,43–50] for LSS and e.g. [51–54] for the CMB.

Our method in [41] executes 20 one-dimensional FFTs to return the 1-loop power spectrum over several decades in

wave number at once at machine-level precision. This exploits spherical symmetry of large-scale structure formation in real space by analytically integrating over orientations. The linear input power spectrum can thereby have an arbitrary functional form as long as it can be represented on a high-resolution, one-dimensional grid that is used for one-dimensional FFTs. In particular, the method can easily resolve the imprint of baryonic acoustic oscillations, BAO, on the initial power spectrum (see Sec. VI A). This is crucial for providing state-of-the-art model predictions for the nonlinear evolution of BAO features in ΛCDM models and extensions thereof.

Our goal in this paper is to generalize the fast fourier transform perturbation theory (FFT-PT) approach introduced in [41] to higher order in large-scale structure perturbation theory, specifically to the 2-loop power spectrum, corresponding to next-to-next-to-leading order in the linear mass density. This generalization is important to test the applicability of the fast FFT-PT framework of [41] beyond 1-loop power spectrum integrals. It should also help to make 2-loop perturbation theory more practically useable, for example to constrain cosmological parameters from a given data set with only little computational cost.

While FFT-PT relies on exact analytical reformulations of the relevant 2-loop integrals, a viable alternative to reduce computational cost is to evaluate approximations of those integrals. As demonstrated by Refs. [55,56], this can be achieved by Taylor expanding around a fiducial cosmological model, or by precomputing integrals for a fiducial cosmology with high precision and then computing corrections for another cosmology with lower precision. The accuracy level and robustness of such approximate methods needs to be checked for every application, e.g. when accounting for halo biasing, redshift space distortions or extensions of the basic ΛCDM model.

Although we share the same motivation and goals with Refs. [55,56], our exact FFT-PT method is technically completely different and therefore complementary in practice, providing a useful path for cross-checks. It would also be interesting to combine the ideas of [55,56] and our method in the future, particularly if the goal is to compute the 2-loop power spectrum robustly for different cosmological parameters at the subpercent level precision that is needed to realize the full scientific potential of future LSS surveys.

For clarity we will focus on the standard 2-loop integrals for the matter power spectrum in SPT. However, our formalism can also handle halo bias, redshift space distortions (RSD), effects from the relative velocity between dark matter and baryons [57], or corrections from the effective field theory of large-scale structure [22,23], because the relevant integrals have the same form as the ones we consider here. For example, halo bias can be included simply by modifying the perturbative F_n kernels that enter the loop integrals (see Sec. VI E), while RSD effects amount to including additional velocity correlators

involving velocity kernels G_n (see Sec. VI F). In principle it should also be possible to generalize the formalism to higher-order statistics beyond the power spectrum. Our method should also work for cosmological models beyond ΛCDM as long as analytical expressions for perturbative kernels exist (see [58] for recent progress in this direction). For models that do not allow for analytical perturbative kernels one instead has to resort to alternative approaches, for example computing kernels fully numerically. While this is possible for subsets of 2-loop contributions by storing kernels on grids [59], it is not clear if fourth or fifth order kernels could be included efficiently in such an approach.

Our paper is organized as follows. To get intuition, we first introduce higher-order corrections to 2-point statistics in a simple perturbative toy model in Sec. II. In Sec. III we generalize this to a subclass of simple 2-loop SPT power spectrum corrections that do not involve inverse Laplacians. We then generalize this to account for a single inverse Laplacian in Sec. IV, and multiple inverse Laplacians in Sec. V. In Sec. VI we comment on the applicability of the method, and extensions to e.g. biased tracers. Finally, we conclude in Sec. VII. Appendices provide background material, derivations, and show how some of the general results simplify further for the special case of scaling universes with power law initial power spectrum.

A. Conventions and notation

Throughout our paper, $\mathbf{k}$ and $\mathbf{q}$ refer to Fourier space, whereas $\mathbf{r}$ and $\mathbf{x}$ refer to position space. We use the following shorthand notation for Fourier space integrals:

$$\int_{\mathbf{q}} \equiv \int \frac{\mathrm{d}^3\mathbf{q}}{(2\pi)^3}. \tag{1}$$

Hats denote unit vectors, e.g. $\hat{\mathbf{q}} = \mathbf{q}/q$, where $q = |\mathbf{q}|$. P_{lin} denotes the linear matter density power spectrum, whereas P_ℓ refers to Legendre polynomials. We sometimes abbreviate indices of spherical harmonics as $\boldsymbol{\ell} = (\ell, m)$ and use the shorthand notation $\sum_{\boldsymbol{\ell}}^{l_{\mathrm{max}}} = \sum_{\ell=0}^{\ell_{\mathrm{max}}} \sum_{m=-\ell}^{\ell}$. Spherical harmonics are normalized so that $\int \mathrm{d}\Omega_{\hat{\mathbf{q}}} Y_{\ell m}(\hat{\mathbf{q}}) Y_{\ell' m'}^*(\hat{\mathbf{q}}) = \delta_{\ell\ell'} \delta_{mm'}$ and $Y_{00}(\hat{\mathbf{q}}) = (4\pi)^{-1/2}$. We highlight the most important results of our paper in boxed equations.

II. PERTURBATIVE CORRECTIONS TO THE 2-POINT CORRELATION FUNCTION

In this section we introduce higher-order corrections to the matter 2-point correlation function in a simple toy model, which is useful to get intuition for the full corrections discussed later.

A. Perturbative 2-point correlation function: Overview of terms in a toy model

The approach of Eulerian standard perturbation theory (SPT) to solve the fluid equations for the large-scale dark

matter overdensity is to expand this overdensity and the velocity perturbatively in the linear overdensity δ_1,

$$\delta(\mathbf{x}) = \sum_{n=1}^{\infty} \delta_n(\mathbf{x}). \tag{2}$$

Here, the nth order contribution δ_n to the full nonlinear overdensity is of order $(\delta_1)^n$. It has a known analytical form that follows from the fluid equations in an expanding universe. The 2-point correlation function or power spectrum of the nonlinear density is then given by summing up contributions at different orders:

$$\langle\delta\delta\rangle = \underbrace{\langle\delta_1\delta_1\rangle}_{\text{tree-level}} + \underbrace{2\langle\delta_1\delta_3\rangle + \langle\delta_2\delta_2\rangle}_{\text{1-loop}}$$
$$+ \underbrace{2\langle\delta_1\delta_5\rangle + 2\langle\delta_2\delta_4\rangle + \langle\delta_3\delta_3\rangle}_{\text{2-loop}} + \underbrace{\mathcal{O}(\delta_1^8)}_{\text{higher loops}}. \tag{3}$$

The first term is the leading-order contribution, which is usually called the tree-level contribution because the corresponding Feynman diagram does not involve any loops. The next two terms are the 1-3 correlation between the linear and third order density, and the 2-2 correlation between the two second order densities. These are next-to-leading order contributions to the power spectrum. The Feynman diagrams of these 1-loop terms involve a single loop. The next three terms, corresponding to 1-5, 2-4 and 3-3 correlations, are next-to-next-to-leading-order terms, corresponding to Feynman diagrams with two loops that will be the focus of our paper.

These 2-loop integrals are typically studied in Fourier instead of position space. This has the advantage that differential operators like gradients or inverse Laplacians turn into analytical expressions of Fourier wave vectors, which are simple to write down and evaluate. However, working in Fourier space comes at the expense of introducing convolution integrals that would be simpler products of fields in position space.

Since both the differential operators in position space and the convolutions in Fourier space represent substantial complications to typical calculations, we start with a simple but unphysical *toy model* where we ignore all differential operators to simplify position space calculations. Specifically, let us assume for a moment that the nth order density is just the nth power of the linear density,

$$\delta_n(\mathbf{x}) \equiv [\delta_1(\mathbf{x})]^n. \tag{4}$$

In this toy model, the 1-3 part of the 1-loop contribution to the 2-point correlation function is

$$\langle\delta_1(\mathbf{x})\,\delta_3(\mathbf{x}')\rangle = 3\,\langle\overline{\delta_1(\mathbf{x})\,\delta_1(\mathbf{x}')}\overline{\delta_1(\mathbf{x}')\delta_1(\mathbf{x}')}\rangle$$
$$= 3\,\xi(r)\xi(0) \tag{5}$$

where the position $\mathbf{x}' \equiv \mathbf{x} + \mathbf{r}$ is separated by a distance r from $\mathbf{x}$. We also defined $\xi(r) = \langle\delta_1(\mathbf{x})\delta_1(\mathbf{x}')\rangle$ as the 2-point correlation function of the linear density, with $\xi(0)$ representing the correlation at zero lag $r = 0$. Similarly, we obtain for the 2-2 contribution to the 2-point correlation function

$$\langle\delta_2(\mathbf{x})\,\delta_2(\mathbf{x}')\rangle = 2\langle\overline{\delta_1(\mathbf{x})\delta_1(\mathbf{x})}\,\overline{\delta_1(\mathbf{x}')\delta_1(\mathbf{x}')}\rangle$$
$$+ \langle\overline{\delta_1(\mathbf{x})\delta_1(\mathbf{x})}\,\overline{\delta_1(\mathbf{x}')\delta_1(\mathbf{x}')}\rangle \tag{6}$$
$$= 2\,[\xi(r)]^2 + [\xi(0)]^2,$$

We can calculate similar expressions for 2-loop contributions in this simple toy model. The 1-5 contribution is given by a linear correlation function at nonzero separation r multiplied by the square of the zero lag term $\xi(0)$,

$$\langle\delta_1(\mathbf{x})\,\delta_5(\mathbf{x}')\rangle = 15\,\langle\overline{\delta_1(\mathbf{x})\,\delta_1(\mathbf{x}')}\overline{\delta_1(\mathbf{x}')\delta_1(\mathbf{x}')}\overline{\delta_1(\mathbf{x}')\delta_1(\mathbf{x}')}\rangle$$
$$= 15\,\xi(r)[\xi(0)]^2. \tag{7}$$

The 2-4 contribution has two qualitatively different contractions,

$$\langle\delta_2(\mathbf{x})\,\delta_4(\mathbf{x}')\rangle = 12\langle\overline{\delta_1(\mathbf{x})\delta_1(\mathbf{x})}\,\overline{\delta_1(\mathbf{x}')\delta_1(\mathbf{x}')}\overline{\delta_1(\mathbf{x}')\delta_1(\mathbf{x}')}\rangle$$
$$+ 3\langle\overline{\delta_1(\mathbf{x})\delta_1(\mathbf{x})}\,\overline{\delta_1(\mathbf{x}')\delta_1(\mathbf{x}')}\overline{\delta_1(\mathbf{x}')\delta_1(\mathbf{x}')}\rangle$$
$$= 12\,[\xi(r)]^2\xi(0) + 3\,[\xi(0)]^3. \tag{8}$$

Finally, the 3-3 contribution is

$$\langle\delta_3(\mathbf{x})\,\delta_3(\mathbf{x}')\rangle = 6\,\langle\overline{\delta_1(\mathbf{x})\delta_1(\mathbf{x})\delta_1(\mathbf{x})}\,\overline{\delta_1(\mathbf{x}')\delta_1(\mathbf{x}')\delta_1(\mathbf{x}')}\rangle$$
$$+ 9\,\langle\overline{\delta_1(\mathbf{x})\delta_1(\mathbf{x})}\overline{\delta_1(\mathbf{x})\,\delta_1(\mathbf{x}')}\overline{\delta_1(\mathbf{x}')\delta_1(\mathbf{x}')}\rangle$$
$$= 6\,[\xi(r)]^3 + 9\,\xi(r)[\xi(0)]^2. \tag{9}$$

In the toy model of Eq. (4), the 1- and 2-loop integrals thus only involve products of the 2-point correlation function $\xi(r)$ and the zero-lag correlation $\xi(0)$. The computational cost of evaluating 1- and 2-loop integrals is therefore trivial in this toy model.

It is not clear, however, if such a simple form of 1- and 2-loop integrals can also be obtained if we work with the full physical nth order density perturbations that involve gradient and inverse Laplacian operators. While this has recently been shown to be the case for 1-loop integrals in [41] (also see [42–44]), it is not clear if 2-loop integrals allow similar simplifications. Addressing this question is the main goal of our paper.

Note that the constant $[\xi(0)]^2$ and $[\xi(0)]^3$ terms in 2-2 and 2-4 correlations are not present if we consider only the connected part of the correlation functions, $\langle AB \rangle_c = \langle AB \rangle - \langle A \rangle \langle B \rangle$, or if we enforce the density to have zero average at each order, $\delta_n = \delta_1^n - \langle \delta_1^n \rangle$.

B. Eulerian fluid and equations of motion

The toy model where the nth order density perturbation is just the linear density raised to the nth power is not physical because it does not solve the equations of motion of DM in an expanding background. We briefly summarize here how to generalize the perturbative expansion so that it solves these equations (see [16] for a review).

The relevant fluid equations can be written as the Fourier transform of the continuity equation,

$$
\dot{\delta}(\mathbf{k}, \tau) + \theta(\mathbf{k}, \tau) = - \int_{\mathbf{k}_1 \mathbf{k}_2} (2\pi)^3 \delta^D(\mathbf{k} - \mathbf{k}_1 - \mathbf{k}_2)
$$
$$
\times \, \alpha(\mathbf{k}_1, \mathbf{k}_2) \delta(\mathbf{k}_1, \tau) \theta(\mathbf{k}_2, \tau), \qquad (10)
$$

and the Fourier transform of the divergence of the Euler equation,

$$
\dot{\theta}(\mathbf{k}, \tau) + \mathcal{H}(\tau)\theta(\mathbf{k}, \tau) + \frac{3}{2}\mathcal{H}(\tau)^2 \Omega_m(\tau) \delta(\mathbf{k}, \tau)
$$
$$
= - \int_{\mathbf{k}_1 \mathbf{k}_2} (2\pi)^3 \delta^D(\mathbf{k} - \mathbf{k}_1 - \mathbf{k}_2) \beta(\mathbf{k}_1, \mathbf{k}_2)
$$
$$
\times \, \theta(\mathbf{k}_1, \tau) \theta(\mathbf{k}_2, \tau), \qquad (11)
$$

where δ is the matter overdensity, $\theta = \nabla \cdot \mathbf{v}$ is the velocity divergence, $\dot{} = d/d\tau$ is the time derivative relative to conformal time, and $\mathcal{H}$ is the conformal Hubble parameter. We have also introduced the abbreviations

$$
\alpha(\mathbf{k}_1, \mathbf{k}_2) = \frac{(\mathbf{k}_1 + \mathbf{k}_2) \cdot \mathbf{k}_2}{k_2^2} = 1 + \frac{1}{k_2^2}(\mathbf{k}_1 \cdot \mathbf{k}_2),
$$
$$
\beta(\mathbf{k}_1, \mathbf{k}_2) = \frac{(\mathbf{k}_1 \cdot \mathbf{k}_2)|\mathbf{k}_1 + \mathbf{k}_2|^2}{2k_1^2 k_2^2}
$$
$$
= \frac{\mathbf{k}_1 \cdot \mathbf{k}_2}{2k_1^2 k_2^2}(k_1^2 + k_2^2 + 2(\mathbf{k}_1 \cdot \mathbf{k}_2)). \qquad (12)
$$

These kernels can be interpreted in position space by noting that multiplication with a wave vector $\mathbf{k}$ corresponds to taking the gradient, whereas multiplication with $\mathbf{k}/k^2$ corresponds to the gradient of the inverse Laplacian, i.e. the gradient of a potential.

The equations of motion can be solved with the perturbative ansatz

$$
\delta = \sum_{n=0}^{\infty} \delta_n, \qquad (13)
$$

where the nth order perturbation in Fourier space is an n-fold convolution of the linear density δ_1 filtered by a (symmetrized) kernel $F_n^{(s)}$,

$$
\delta_n(\mathbf{k}) = F_n^{(s)} \delta_1 * \cdots * \delta_1, \qquad (14)
$$

or writing this more explicitly,

$$
\delta_n(\mathbf{k}) = \int_{\mathbf{q}_1 \cdots \mathbf{q}_n} (2\pi)^3 \delta_D(\mathbf{k} - \mathbf{q}_1 \cdots - \mathbf{q}_n)
$$
$$
\times F_n^{(s)}(\mathbf{q}_1, \ldots, \mathbf{q}_n)\delta_1(\mathbf{q}_1) \cdots \delta_1(\mathbf{q}_n). \qquad (15)
$$

A similar expression follows for the velocity divergence θ.

Explicit expressions for the $F_n^{(s)}$ kernels can be obtained from recursion relations that follow from the equations of motion; see Appendix A. For our purposes, however, we only need to know the general form of the F_n filter kernels. This is determined by the operators appearing in the fluid equations of motion, involving e.g. gradients and inverse Laplacians. Indeed, the nth order kernel $F_n^{(s)}(\mathbf{q}_1, \ldots, \mathbf{q}_n)$ involves only sums of products of the following simple "building block" operators:

$$
F_n^{(s)}(\mathbf{q}_1, \ldots, \mathbf{q}_n)
$$
$$
\sim \left\{ |\mathbf{q}_i|^{n_i}, (\hat{\mathbf{q}}_i \cdot \hat{\mathbf{q}}_j)^{\ell_i}, \frac{1}{|s_1\mathbf{q}_1 + \cdots + s_n\mathbf{q}_n|^2} \right\}, \qquad (16)
$$

where n_i are integers, l_i are non-negative integers, and $s_i \in \{-1, 0, 1\}$. The last operator in Eq. (16) corresponds to an inverse Laplacian. The velocity kernels $G_n^{(s)}$ involve the same building blocks.

The simple toy model calculation from Sec. II A thus needs to be refined by including these building blocks for the nth order perturbation in Fourier space. Except for the inverse Laplacians, which require more work and will be discussed in a later section, this is relatively straightforward, as we will show next.

III. 2-LOOP POWER SPECTRUM CONTRIBUTIONS WITHOUT INVERSE LAPLACIANS

In this section we discuss contributions to the 2-loop matter power spectrum in Eulerian standard perturbation theory (SPT) that do not involve inverse Laplacians. Sections IV and V will generalize the results to account for such inverse Laplacians.

The form of the 2-loop corrections in full SPT is rather similar to the simple toy model from the last section. The final expressions therefore have a similar form to above, involving zero-lag terms $\xi(0)$ and correlation terms $\xi(r)$ at nonzero separation r. This can also be seen from the diagrammatic representation of the 2-loop integrals in Fig. 1, where "tadpole" subdiagrams (red dashed) lead to zero-lag terms $\xi(0)$ and "connector" subdiagrams (blue) lead to correlation terms $\xi(r)$.
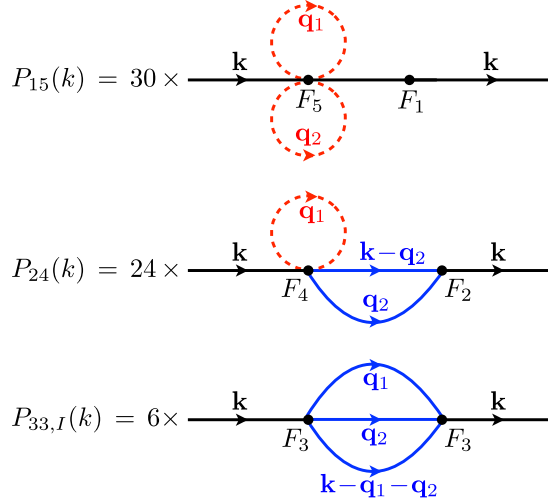
FIG. 1. Diagrammatic representation of nontrivial 2-loop contributions to the dark matter power spectrum in standard Eulerian perturbation theory. Tadpole subdiagrams (red dashed) are evaluated at the same point, leading to zero-lag correlations $\xi(0)$. "Connector" subdiagrams (blue) are evaluated at two different points, leading to correlations $\xi(r)$ at nonzero separation r.

A. 1-5 correlations

We start with the 1-5 contribution to the power spectrum that arises from the correlation between the linear and fifth-order density. From the toy model result of Eq. (7) and the diagram in Fig. 1 we expect this to be of the form $\xi(r)[\xi(0)]^2$, or $P_{\rm lin}(k)[\xi(0)]^2$ in Fourier space. Explicitly, the 1-5 correlation in Fourier space is

$$
\begin{aligned}
P_{15}(k) &= 30 \left\langle \overline{\delta_1 F_5^{(s)} \delta_1} * \overline{\delta_1 * \delta_1} * \overline{\delta_1 * \delta_1} \right\rangle \\
&= 30\, P_{\rm lin}(k) \int_{\mathbf{q}_1 \mathbf{q}_2} F_5^{(s)}(\mathbf{k}, \mathbf{q}_1, -\mathbf{q}_1, \mathbf{q}_2, -\mathbf{q}_2) \\
&\quad \times P_{\rm lin}(q_1) P_{\rm lin}(q_2).
\end{aligned}
\tag{17}
$$

The prefactor arises from 15 possibilities to form the contraction multiplied by two because $\langle \delta_1 \delta_5 \rangle = \langle \delta_5 \delta_1 \rangle$. The F_5 kernel consists of the building block operators listed in Eq. (16), and its angular structure can be parametrized by angular products between the arguments of the F_5 kernel, i.e. the edges attached to the F_5 vertex in Fig. 1. The most general form of such 1-5 contributions, ignoring inverse Laplacians for now, reduces to the following simple and fast-to-evaluate form (see endnote [60])

$$
\begin{aligned}
k^{n_0} P_{\rm lin}(k) &\int_{\mathbf{q}_1 \mathbf{q}_2} (\hat{\mathbf{q}}_1 \cdot \hat{\mathbf{q}}_2)^{\ell_0} (\hat{\mathbf{k}} \cdot \hat{\mathbf{q}}_1)^{\ell_1} (\hat{\mathbf{k}} \cdot \hat{\mathbf{q}}_2)^{\ell_2} \\
&\times q_1^{n_1} P_{\rm lin}(q_1) q_2^{n_2} P_{\rm lin}(q_2) \\
&= k^{n_0} P_{\rm lin}(k) \mathcal{M}_0(\ell_0, \ell_1, \ell_2) \xi_{n_1}^0(0) \xi_{n_2}^0(0).
\end{aligned}
\tag{18}
$$

As expected from the toy model Eq. (7), the linear power spectrum $P_{\rm lin}(k)$ is multiplied by a k-independent product of two zero-lag correlations,

$$
\xi_n^0(0) = \int_0^\infty \frac{dq}{2\pi^2} q^{2+n} P_{\rm lin}(q).
\tag{19}
$$

These are fast to evaluate, either as a 1D integral over the linear power spectrum or by selecting the $r = 0$ entry of a 1D Hankel transform with $l = 0$. The coupling factor $\mathcal{M}_0$ in Eq. (18) is a number defined by Eq. (B1) in Appendix B. The first few values are given in Table I.

B. 2-4 correlations

We proceed with 2-4 correlations. From the toy model result of Eq. (8), we expect them to be of the form $\xi(0)[\xi(r)]^2$ and $[\xi(0)]^3$, where only the former depends on the separation and contributes to the Fourier space power spectrum at nonzero wave number. Explicitly, this 2-4 contribution to the power spectrum is

$$
\begin{aligned}
P_{24}(k) &= 24 \left\langle (F_4^{(s)} \overline{\delta_1 * \delta_1} * \overline{\delta_1 * \delta_1}) (F_2^{(s)} \overline{\delta_1 * \delta_1}) \right\rangle \\
&= 24 \int_{\mathbf{q}_1 \mathbf{q}_2} F_4^{(s)}(\mathbf{q}_1, -\mathbf{q}_1, \mathbf{q}_2, \mathbf{k}-\mathbf{q}_2)\, F_2^{(s)}(\mathbf{q}_2, \mathbf{k}-\mathbf{q}_2) \\
&\quad \times P_{\rm lin}(q_1)\, P_{\rm lin}(q_2)\, P_{\rm lin}(|\mathbf{k}-\mathbf{q}_2|).
\end{aligned}
\tag{20}
$$

Introducing $\mathbf{q}_3 \equiv \mathbf{k} - \mathbf{q}_2$ with a Dirac delta, we obtain for 2-4 contributions without inverse Laplacians the following fast expression (see endnote [61])

$$
\begin{aligned}
\int_{\mathbf{q}_1 \mathbf{q}_2 \mathbf{q}_3} &(2\pi)^3 \delta_D(\mathbf{q}_3 - (\mathbf{k}-\mathbf{q}_2))(\hat{\mathbf{q}}_2 \cdot \hat{\mathbf{q}}_3)^{\ell_1}(\hat{\mathbf{q}}_1 \cdot \hat{\mathbf{q}}_3)^{\ell_2} \\
&\times (\hat{\mathbf{q}}_1 \cdot \hat{\mathbf{q}}_2)^{\ell_3} q_1^{n_1} P_{\rm lin}(q_1) q_2^{n_2} P_{\rm lin}(q_2) q_3^{n_3} P_{\rm lin}(q_3) \\
&= \xi_{n_1}^0(0)(4\pi)^{3/2} \int_0^\infty dr\, r^2 j_0(kr) \\
&\times \sum_{L=0}^{\ell_1 + \min(\ell_2, \ell_3)} \mathcal{M}_1(\ell_1, \ell_2, \ell_3; L) \xi_{n_2}^L(r) \xi_{n_3}^L(r).
\end{aligned}
\tag{21}
$$

The right-hand side is similar to the $\xi(0)[\xi(r)]^2$ structure expected from the toy model result of Eq. (8) and the diagram in Fig. 1. The radial integral is the result of the angle-averaged 3D Fourier transform of $[\xi(r)]^2$; see Eq. (G12). This integral is weighted by a spherical Bessel function j_ℓ and is therefore a 1D Hankel transform. This can be evaluated efficiently and robustly with a 1D FFT using FFTLog [62].

In Eq. (21) we defined a generalized correlation function ξ_n^ℓ as

$$\xi_n^\ell(r) = \int_0^\infty \frac{dq}{2\pi^2} q^{2+n} j_l(qr) P_{\text{lin}}(q). \qquad (22)$$

This is related to the 2-point correlation between the linear density and a derivative or inverse Laplacian of the linear density [41]. Each $\xi_n^\ell(r)$ is a 1D Hankel transform of the linear power spectrum and can therefore again be computed with a 1D FFT. The right-hand side of Eq. (21) can therefore be evaluated using only 1D FFTs. The coupling factors $\mathcal{M}_1$ are defined in Eq. (B3), with some example values given in Table I.

C. 3-3 correlations

The last contribution to the 2-loop power spectrum is the 3-3 correlation of two third-order densities. From the toy model results of Eq. (9) we expect contributions of the forms $[\xi(r)]^3$ and $\xi(r)[\xi(0)]^2$. It is well known that the latter term reduces to a term proportional to $[P_{13}(k)]^2/P_{\text{lin}}(k)$, i.e. it can be obtained directly from the P_{13} 1-loop integral. We therefore only consider the nontrivial 3-3 term which is of the form $[\xi(r)]^3$. We expect that this part of the nontrivial 3-3 contribution to the power spectrum should become a 3D Fourier transform or 1D Hankel transform of $[\xi(r)]^3$. Indeed, the nontrivial 3-3 power spectrum is

$$
\begin{aligned}
P_{33,I}(k) &= 6 \left\langle (F_3^{(s)} \overbrace{\delta_1 * \delta_1 * \delta_1})(F_3^{(s)} \overbrace{\delta_1 * \delta_1 * \delta_1}) \right\rangle \\
&= 6 \int_{\mathbf{q}_1 \mathbf{q}_2 \mathbf{q}_3} (2\pi)^3 \delta_D(\mathbf{k} - \mathbf{q}_1 - \mathbf{q}_2 - \mathbf{q}_3) \qquad (23) \\
&\quad \times [F_3^{(s)}(\mathbf{q}_1, \mathbf{q}_2, \mathbf{q}_3)]^2 P_{\text{lin}}(q_1) P_{\text{lin}}(q_2) P_{\text{lin}}(q_3)
\end{aligned}
$$

and contributions to this without inverse Laplacians reduce to (see endnote [63])

$$
\begin{aligned}
&\int \frac{d\Omega_{\hat{\mathbf{k}}}}{4\pi} \int_{\mathbf{q}_1 \mathbf{q}_2 \mathbf{q}_3} (2\pi)^3 \delta_D(\mathbf{k} - \mathbf{q}_1 - \mathbf{q}_2 - \mathbf{q}_3) \\
&\quad \times (\hat{\mathbf{q}}_2 \cdot \hat{\mathbf{q}}_3)^{\ell_1} (\hat{\mathbf{q}}_1 \cdot \hat{\mathbf{q}}_3)^{\ell_2} (\hat{\mathbf{q}}_1 \cdot \hat{\mathbf{q}}_2)^{\ell_3} \prod_{i=1}^3 q_i^{n_i} P_{\text{lin}}(q_i) \\
&= 4\pi \int_0^\infty dr\, r^2 j_0(kr) \left[\sum_{L_1=0}^{\ell_2+\ell_3} \sum_{L_2=0}^{\ell_1+\ell_3} \sum_{L_3=0}^{\ell_1+\ell_2} \right. \\
&\quad \times \left. \mathcal{M}_3(\ell_1, \ell_2, \ell_3; L_1, L_2, L_3) \xi_{n_1}^{L_1}(r) \xi_{n_2}^{L_2}(r) \xi_{n_3}^{L_3}(r) \right] \qquad (24)
\end{aligned}
$$

As expected, this is a 1D Hankel transform of a finite sum of triple products of linear correlation functions $\xi_n^\ell(r)$, which can be computed using only 1D FFTs.

The right-hand side of Eq. (24) involves the coupling factor $\mathcal{M}_3$ defined by Eq. (B5). For $\ell_1 \le \ell_2 \le \ell_3 \le 1$ the only nonzero couplings to L_i are listed in Table I. For example, for $(\ell_1, \ell_2, \ell_3) = (0, 1, 1)$ only two couplings are nonzero, $(L_1, L_2, L_3) = (0, 1, 1)$ and $(2, 1, 1)$, so we only need to compute $\xi_{n_1}^0$, $\xi_{n_1}^2$, $\xi_{n_2}^1$ and $\xi_{n_3}^1$ and one additional 1D

TABLE I. The angular structure of 2-loop integrands leads to coupling factors $\mathcal{M}_n$ between three angular momenta (ℓ_1, ℓ_2, ℓ_3) and n angular momenta L. The table shows all nonzero coupling factors $\mathcal{M}_0(\ell_1, \ell_2, \ell_3)$ for $\ell_i \le 2$, $\mathcal{M}_1(\ell_1, \ell_2, \ell_3; L)$ for $l_i \le 1$, as well as $\mathcal{M}_2(\ell_1, \ell_2, \ell_3; L, L')$ and $\mathcal{M}_3(\ell_1, \ell_2, \ell_3; L_1, L_2, L_3)$ for $\ell_1 \le \ell_2 \le \ell_3 \le 1$. See Appendix B for definitions of these factors.

(ℓ_1, ℓ_2, ℓ_3)		$\mathcal{M}_0$
(0, 0, 0)		1
(0, 0, 2)		1/3
(0, 2, 0)		1/3
(0, 2, 2)		1/9
(1, 1, 1)		1/9
(2, 0, 0)		1/3
(2, 0, 2)		1/9
(2, 2, 0)		1/9
(2, 2, 2)		11/225

(ℓ_1, ℓ_2, ℓ_3)	L	$\mathcal{M}_1$
(0, 0, 0)	0	1
(0, 1, 1)	1	−1/3
(1, 0, 0)	1	−1
(1, 1, 1)	0	1/9
(1, 1, 1)	2	2/9

(ℓ_1, ℓ_2, ℓ_3)	(L, L')	$\mathcal{M}_2$
(0, 0, 0)	(0, 0)	1
(0, 0, 1)	(1, 0)	−1
(0, 1, 1)	(0, 1)	−1/3
(0, 1, 1)	(2, 1)	−2/3
(1, 1, 1)	(0, 0)	1/9
(1, 1, 1)	(0, 2)	2/9
(1, 1, 1)	(2, 0)	2/9
(1, 1, 1)	(2, 2)	4/9

(ℓ_1, ℓ_2, ℓ_3)	(L_1, L_2, L_3)	$\mathcal{M}_3$
(0, 0, 0)	(0, 0, 0)	1
(0, 0, 1)	(1, 1, 0)	−1
(0, 1, 1)	(0, 1, 1)	−1/3
(0, 1, 1)	(2, 1, 1)	2/3
(1, 1, 1)	(0, 0, 0)	1/9
(1, 1, 1)	(0, 2, 2)	2/9
(1, 1, 1)	(2, 0, 2)	2/9
(1, 1, 1)	(2, 2, 0)	2/9
(1, 1, 1)	(2, 2, 2)	−2/9

Hankel transform to go back to Fourier space, requiring five 1D FFTs in total.

IV. SINGLE INVERSE LAPLACIAN IN THE 2-LOOP POWER SPECTRUM

For simplicity, we have ignored inverse Laplacian operators so far. In fact, however, they do appear in the perturbative solutions for the DM fluid because the continuity equation (10) and the Euler equation (11) involve

the gradient of the velocity divergence potential, $\nabla_i \nabla^{-2}\theta$. When solving the equations perturbatively, we therefore encounter expressions like the inverse Laplacian of composite quadratic fields, e.g. $\nabla^{-2}\theta^{(2)} \sim \nabla^{-2}[\delta_1^2]$. In Fourier space, this is represented by terms like $|\mathbf{q}_1 + \mathbf{q}_2|^{-2}$ (this can also be seen from the recursion relations for the perturbative Fourier space F_n kernels; see Appendix A). Such Fourier space factors can render the integrand of loop integrals nonseparable in the integration variables $\mathbf{q}_1$ and $\mathbf{q}_2$, so that the integrand cannot be written as a function of $\mathbf{q}_1$ multiplied by a function of $\mathbf{q}_2$. This may seem problematic for the approach used in the previous section, because the 2-loop integrals do not straightforwardly split into an integral over $\mathbf{q}_1$ multiplied by an integral over $\mathbf{q}_2$. In this section we show that it is still possible to reduce 2-loop integrals with a single inverse Laplacian to 1D Hankel transforms that allow fast evaluation. The more complicated case involving multiple inverse Laplacians will be discussed in Sec. V.

A. 1-5 correlations with inverse Laplacians: Products of two correlation functions

1. Simple example

We first generalize the 1-5 correlations from Eqs. (7) and (18) to the case with a nontrivial inverse Laplacian. To see how the inverse Laplacian can look like in Fourier space, consider for example

$$\int \mathrm{d}^3\mathbf{r}\, e^{i\mathbf{k}\cdot\mathbf{r}} \langle \overline{\delta_1(\mathbf{x})\,\delta_1(\mathbf{x}')}\overline{\delta_1(\mathbf{x}')\delta_1(\mathbf{x}')}\nabla^{-2}[\delta_1(\mathbf{x}')\delta_1(\mathbf{x}')]\rangle$$
$$= -P_{\mathrm{lin}}(k)\int_{\mathbf{q}_1\mathbf{q}_2}\frac{1}{|\mathbf{q}_1+\mathbf{q}_2|^2}P_{\mathrm{lin}}(q_1)P_{\mathrm{lin}}(q_2),$$
(25)

where the right-hand side follows from

$$\langle \overline{\delta_1(\mathbf{x})\delta_1(\mathbf{x}')}\rangle = \int_{\mathbf{q}}e^{-i\mathbf{q}\cdot(\mathbf{x}-\mathbf{x}')}P_{\mathrm{lin}}(q).$$
(26)

The particular inverse Laplacian in Eq. (25) thus turns into $-|\mathbf{q}_1+\mathbf{q}_2|^{-2}$ in Fourier space. To evaluate the resulting 2-loop integral over $\mathbf{q}_1$ and $\mathbf{q}_2$ efficiently, we introduce $\mathbf{q}_3 = \mathbf{q}_1 + \mathbf{q}_2$ with a Dirac delta, integrate out all orientations and use Eq. (G13) to obtain

$$\int_{\mathbf{q}_1\mathbf{q}_2}\frac{P_{\mathrm{lin}}(q_1)P_{\mathrm{lin}}(q_2)}{|\mathbf{q}_1+\mathbf{q}_2|^2} = \int_0^\infty \mathrm{d}r\, r\xi_0^0(r)\xi_0^0(r).$$
(27)

This is just a radial integral over the product of two correlation functions, which can be evaluated very efficiently.

2. General case

The most general form of the inverse Laplacian can be deduced from the arguments of the F_5 kernel in Eq. (18) and the form of the kernel recursion relations in Appendix A; it is given by $|s_0\mathbf{k} + s_1\mathbf{q}_1 + s_2\mathbf{q}_2|^{-2}$, with parameters $s_i \in \{-1, 0, 1\}$ that parametrize on which fields the inverse Laplacian acts. Allowing also for nontrivial angular dependence in the integrand that arises from gradient operators ∇_i, we obtain for the most general 1-5 contribution to the power spectrum (see endnote [64] for a derivation):

$$
\begin{aligned}
&k^{n_0}P_{\mathrm{lin}}(k)\int\frac{\mathrm{d}\Omega_{\hat{\mathbf{k}}}}{4\pi}\int_{\mathbf{q}_1\mathbf{q}_2}(\hat{\mathbf{q}}_1\cdot\hat{\mathbf{q}}_2)^{\ell_0}(\hat{\mathbf{k}}\cdot\hat{\mathbf{q}}_1)^{\ell_1}\\
&\times(\hat{\mathbf{k}}\cdot\hat{\mathbf{q}}_2)^{\ell_2}\frac{q_1^{n_1}P_{\mathrm{lin}}(q_1)q_2^{n_2}P_{\mathrm{lin}}(q_2)}{|s_0\mathbf{k}+s_1\mathbf{q}_1+s_2\mathbf{q}_2|^2}\\
&= k^{n_0}P_{\mathrm{lin}}(k)\sum_{L_0=0}^{\ell_1+\ell_2}(\mathrm{sgn}s_0)^{L_0}\int_0^\infty \mathrm{d}r r j_{L_0}(|s_0|kr)\\
&\times\left[\sum_{L_1=0}^{\ell_0+\ell_1}\sum_{L_2=0}^{\ell_0+\ell_2}\mathcal{M}_3(\ell_0,\ell_1,\ell_2;L_0,L_2,L_1)\right.\\
&\left.\times\xi_{n_1,s_1}^{L_1}(r)\xi_{n_2,s_2}^{L_2}(r)\right].
\end{aligned}
$$
(28)

The right-hand side of Eq. (28) is given by 1D Hankel transforms of products of two correlation functions ξ, which are themselves given by 1D Hankel transforms of the linear power spectrum. Thus, using Eqs. (18) and (28), the calculation of the full $P_{15}(k)$ contribution to the 2-loop power spectrum at all k can be obtained by a sequence of 1D Hankel transforms, which are fast to compute with 1D FFTs using FFTLog [62].

Note that Eq. (28) is only meant to be applied for cases with nontrivial inverse Laplacians where at least two of s_0, s_1, s_2 are nonzero, because otherwise there is no nonseparable denominator and Eq. (18) can be applied instead. The right-hand side of Eq. (28) involves the coupling factor $\mathcal{M}_3$ defined in Eq. (B5) and listed in Table I. It also involves the generalized correlation functions

$$\xi_{n,s}^\ell(r) \equiv (\mathrm{sgn}s)^l\int_0^\infty\frac{\mathrm{d}q}{2\pi^2}q^{2+n}P_{\mathrm{lin}}(q)j_l(|s|qr),$$
(29)

where $s \in \{-1, 0, 1\}$. They reduce to the usual correlations $\xi_n^\ell(r)$ for $|s| = 1$ and to zero-lag terms $\xi_n^0(0)$ for $s = 0$, because $j_l(0) = \delta_{l0}$. In the special case $\ell_i = n_i = s_0 = 0$ and $s_1 = s_2 = 1$, Eq. (28) reduces to the simple result of Eq. (27).

B. 2-4 correlations with inverse Laplacians

1. Simple example

We now turn to 2-4 correlations including inverse Laplacians. Our main idea to evaluate these 2-loop integrals

is to split them into nested 1-loop integrals that are much simpler to evaluate. For clarity we introduce this approach first for a simple special case in this section, discussing the fully general case in the subsequent section and in Appendix C.

The special case we consider is given by the first contraction of Eq. (8) if we include an inverse Laplacian acting on the squared linear density as

$$\int d^3 r\, e^{i\mathbf{k}\cdot\mathbf{r}} \left\langle \overline{\delta_1(\mathbf{x})\underline{\delta_1(\mathbf{x})}\,\delta_1(\mathbf{x}')\underline{\delta_1(\mathbf{x}')}\nabla^{-2}\big[\delta_1(\mathbf{x}')\delta_1(\mathbf{x}')\big]}\right\rangle$$
$$= -\int_{\mathbf{q}_1\mathbf{q}_2} \frac{P_{\mathrm{lin}}(q_1)\,P_{\mathrm{lin}}(q_2)\,P_{\mathrm{lin}}(|\mathbf{k}-\mathbf{q}_2|)}{|\mathbf{q}_1+\mathbf{q}_2|^2},$$

$$(30)$$

where the right-hand side follows from Eq. (26). To speed up evaluation, the main idea is now to write the 2-loop integral (30) as an outer $\mathbf{q}_2$-integral over an inner tadpole integral over $\mathbf{q}_1$:

$$\int_{\mathbf{q}_1\mathbf{q}_2} \frac{P_{\mathrm{lin}}(q_1)P_{\mathrm{lin}}(q_2)P_{\mathrm{lin}}(|\mathbf{k}-\mathbf{q}_2|)}{|\mathbf{q}_1+\mathbf{q}_2|^2}$$
$$= \int_{\mathbf{q}_2} P_{\mathrm{lin}}(q_2)\underbrace{\left[\int_{\mathbf{q}_1} \frac{P_{\mathrm{lin}}(q_1)}{|\mathbf{q}_1+\mathbf{q}_2|^2}\right]}_{P_{\mathrm{tadpole}}(q_2)} P_{\mathrm{lin}}(|\mathbf{k}-\mathbf{q}_2|). \quad (31)$$

This reduces the 2-loop integral to two nested 1-loop integrals that are easy to evaluate. In the diagrammatic representation of Fig. 1, this corresponds to evaluating the red tadpole subdiagram first, and then using the result to compute the blue subdiagram connecting the F_4 and F_2 vertices.

To see more specifically how Eq. (31) simplifies numerical evaluation, we write the inner tadpole integral as (see endnote [65])

$$P_{\mathrm{tadpole}}(q_2) = \int_0^\infty dr\, r j_0(q_2 r)\xi_0^0(r). \quad (32)$$

Then, we can evaluate the Fourier space convolution over $\mathbf{q}_2$ in Eq. (31) as a product in position space, obtaining

$$\int_{\mathbf{q}_1\mathbf{q}_2} \frac{P_{\mathrm{lin}}(q_1)P_{\mathrm{lin}}(q_2)P_{\mathrm{lin}}(|\mathbf{k}-\mathbf{q}_2|)}{|\mathbf{q}_1+\mathbf{q}_2|^2}$$
$$= 4\pi \int_0^\infty dr\, r^2 j_0(kr)\xi_0^0(r)\mathcal{T}(r). \quad (33)$$

This is a 1D Hankel transform of the product between the linear correlation function $\xi_0^0(r)$ and the 4-point-like correlation $\mathcal{T}(r)$. The latter is defined as a 1D Hankel transform of the product of the linear power spectrum P_{lin} and the tadpole integral P_{tadpole}:

$$\mathcal{T}(r) \equiv \int_0^\infty \frac{dq_2}{2\pi^2} q_2^2 j_0(q_2 r)P_{\mathrm{lin}}(q_2)P_{\mathrm{tadpole}}(q_2). \quad (34)$$

Using Eq. (33), the 2-loop integral of Eq. (30) can be computed from a given linear power spectrum with four 1D Hankel transforms in total, which is extremely fast. Similar reductions of 2-loop integrals to two nested 1-loop integrals are also used in other contexts to simplify their evaluation; see e.g. [66] for examples in quantum field theory.

2. General case

The 2-loop integral (30) from the last section is a special case in the sense that the integrand does not contain nontrivial angular dependence from terms like e.g. $\hat{\mathbf{q}}_1\cdot\hat{\mathbf{q}}_2$. One of the main results of our paper is that the FFT-PT approach still works if such nontrivial angular dependence is included in the integrand. While this leads to additional coupling factors, the general strategy is the same as in the last section, i.e. we split the 2-loop integral into two nested 1-loop integrals that can be evaluated as 1D Hankel transforms. This is discussed in detail in Appendix C. The final results for the nontrivial 2-4 correlations, given by Eqs. (C8) and (C11), involve only 1D Hankel transforms, which can be evaluated efficiently with a finite number of 1D FFTs using FFTLog [62].

C. 3-3 correlations with inverse Laplacians: ξ times transformed ξ^2

1. Simple example

We finally turn to the last remaining contribution to the 2-loop power spectrum arising from nontrivial 3-3 correlations. These involve for example an inverse Laplacian acting on two linear densities in Eq. (9) as follows:

$$\int d^3 r\, e^{i\mathbf{k}\cdot\mathbf{r}} \left\langle \overline{\delta_1(\mathbf{x})\overline{\delta_1(\mathbf{x})\underline{\delta_1(\mathbf{x})}\,\delta_1(\mathbf{x}')}\nabla^{-2}\big[\underline{\delta_1(\mathbf{x}')}\delta_1(\mathbf{x}')\big]}\right\rangle$$
$$= -\int_{\mathbf{q}_1\mathbf{q}_2} \frac{P_{\mathrm{lin}}(q_1)P_{\mathrm{lin}}(q_2)P_{\mathrm{lin}}(|\mathbf{k}-\mathbf{q}_1-\mathbf{q}_2|)}{|\mathbf{q}_1+\mathbf{q}_2|^2}.$$

$$(35)$$

Again, the inverse Laplacian turns into $-|\mathbf{q}_1+\mathbf{q}_2|^{-2}$ in Fourier space. This 2-loop integral can be simplified to (see Appendix E 1)

$$\int \frac{d\Omega_{\hat{\mathbf{k}}}}{4\pi} \int_{\mathbf{q}_1\mathbf{q}_2} \frac{P_{\mathrm{lin}}(q_1)P_{\mathrm{lin}}(q_2)P_{\mathrm{lin}}(|\mathbf{k}-\mathbf{q}_1-\mathbf{q}_2|)}{|\mathbf{q}_1+\mathbf{q}_2|^2}$$
$$= (4\pi)^4 \int_0^\infty dr\, r^2 j_0(kr)\xi_0^0(r)\mathbb{T}(r). \quad (36)$$

This is the Hankel transform of the product of the linear correlation function $\xi_0^0(r)$ and the 4-point like quantity $\mathbb{T}(r)$ defined by

$$\mathbb{T}(r) = \int_0^\infty \frac{dq}{2\pi^2} j_0(qr)\int_0^\infty dr''(r'')^2 j_0(qr'')[\xi_0^0(r'')]^2. \quad (37)$$

The latter is obtained by squaring the linear correlation function in position space, transforming the result to Fourier space using a Hankel transform, dividing by q^2, and transforming back to position space with another Hankel transform. Therefore, the 2-loop integral of Eq. (36) is essentially given by ξ times a transform of ξ^2. This is extremely numerically efficient.

2. General case

The most general form of integrals contributing to nontrivial 3-3 correlations follows by also including scalar products in the integrand, and introducing $\mathbf{k} - \mathbf{q}_1 - \mathbf{q}_2 = \mathbf{q}_3$ (see endnote [67] and Appendix E 2):

$$
\begin{aligned}
&\int \frac{d\Omega_{\hat{\mathbf{k}}}}{4\pi} \int_{\mathbf{q}_1\mathbf{q}_2\mathbf{q}_3} (2\pi)^3 \delta_D(\mathbf{k} - \mathbf{q}_1 - \mathbf{q}_2 - \mathbf{q}_3) \\
&\times (\hat{\mathbf{q}}_2 \cdot \hat{\mathbf{q}}_3)^{\ell_1} (\hat{\mathbf{q}}_1 \cdot \hat{\mathbf{q}}_3)^{\ell_2} (\hat{\mathbf{q}}_1 \cdot \hat{\mathbf{q}}_2)^{\ell_3} \frac{1}{|\mathbf{q}_1 + \mathbf{q}_2|^{n_4}} \\
&\times q_1^{n_1} P_{\mathrm{lin}}(q_1) q_2^{n_2} P_{\mathrm{lin}}(q_2) q_3^{n_3} P_{\mathrm{lin}}(q_3) \\
&= (4\pi)^4 \int_0^\infty dr\, r^2 j_0(kr) \sum_{L_3=|\ell_1-\ell_2|}^{\ell_1+\ell_2} \\
&\times \xi_{n_3}^{L_3}(r) \mathbb{T}_{L_3}^{\ell_1\ell_2\ell_3,n_1n_2n_4}(r).
\end{aligned} \tag{38}
$$

The right-hand side is a 1D Hankel transform of a sum of products between linear correlation functions $\xi(r)$ and the 4-point-like quantity $\mathbb{T}(r)$. The latter is defined by applying two subsequent 1D Hankel transforms to a product of two correlation functions $\xi(r)$:

$$
\begin{aligned}
&\mathbb{T}_{L_3}^{\ell_1\ell_2\ell_3,n_1n_2n_4}(r) \\
&\equiv \int_0^\infty \frac{dq}{2\pi^2} q^{2-n_4} j_{L_3}(qr) \left\{ \int_0^\infty dr''(r'')^2 j_{L_3}(qr'') \right. \\
&\times \left[\sum_{L_1=|\ell_2-\ell_3|}^{\ell_2+\ell_3} \sum_{L_2=|\ell_1-\ell_3|}^{\ell_1+\ell_3} \mathcal{M}_3(\ell_1,\ell_2,\ell_3;L_1,L_2,L_3) \right. \\
&\left. \left. \times \xi_{n_1}^{L_1}(r'') \xi_{n_2}^{L_2}(r'') \right] \right\},
\end{aligned} \tag{39}
$$

where the coupling factor $\mathcal{M}_3$ from Eq. (B5) restricts the sums to be finite.

The general 3-3 correlation of Eq. (38) can thus be evaluated with a finite number of 1D Hankel transforms. The structure is similar to the $[\xi(r)]^3$ structure obtained for 3-3 correlations without inverse Laplacians in Eqs. (9) and (24), but the outer-most integral in Eq. (39) effectively applies an inverse Laplacian to the product of two correlation functions $\xi(r)$ as expected from the contractions in Eq. (35) and the simple example of Eq. (36).

V. MULTIPLE INVERSE LAPLACIANS

Unfortunately, the full 2-loop power spectrum also involves contributions that have multiple nontrivial inverse Laplacians, corresponding to multiple nonseparable denominators in 2-loop integrands. Since they involve 3d wave vectors one cannot simply separate the denominators using a partial fraction decomposition and then apply the machinery laid out in the last sections. Instead, we follow a somewhat different approach than in the rest of the paper. This reduces contributions with multiple nontrivial inverse Laplacians to low-dimensional radial integrals. We explicitly show this for the case of trivial numerators in the Fourier space integrals and indicate how more complicated numerators could in principle be generated from this.

A. 1-5 correlations

Based on explicit calculation of the F_5 kernel that enters 1-5 contributions to the power spectrum, we consider integrals of the general form

$$
\begin{aligned}
I_{15}(k,\boldsymbol{\alpha},\boldsymbol{\beta}) &= \int_{\mathbf{q}_1\mathbf{q}_2} \frac{e^{i\boldsymbol{\alpha}\cdot\mathbf{q}_1} e^{i\boldsymbol{\beta}\cdot\mathbf{q}_2}}{q_1^{2n_1}|\mathbf{k}+\mathbf{q}_1|^{2n_1'} q_2^{2n_2}|\mathbf{k}+\mathbf{q}_2|^{2n_2'}} \\
&\times \frac{P_{\mathrm{lin}}(q_1) P_{\mathrm{lin}}(q_2) P_{\mathrm{lin}}(k)}{|\mathbf{q}_1+\mathbf{q}_2|^{2n_3}|\mathbf{k}+\mathbf{q}_1+\mathbf{q}_2|^{2n_3'}},
\end{aligned} \tag{40}
$$

where $n_i, n_i' \leq 2$ and we introduced parameters $\boldsymbol{\alpha}$ and $\boldsymbol{\beta}$. Nontrivial numerators can be generated by computing I_{15} and taking appropriate derivatives with respect to $\boldsymbol{\alpha}$ and $\boldsymbol{\beta}$ evaluated at zero, although we do not explicitly do this here. Introducing a helper variable for $\mathbf{k} + \mathbf{q}_1 + \mathbf{q}_2$ with a Dirac delta, Eq. (40) reduces to

$$
\begin{aligned}
I_{15}(k,\boldsymbol{\alpha},\boldsymbol{\beta}) &= P_{\mathrm{lin}}(k) \int d^3r\, e^{i\mathbf{k}\cdot\mathbf{r}} \Xi_{n_3'n_3}^{(0)}(\mathbf{r},\mathbf{k}) \\
&\times \Xi_{n_1n_1'}^{(1)}(\mathbf{r}+\boldsymbol{\alpha},\mathbf{k}) \Xi_{n_2n_2'}^{(1)}(\mathbf{r}+\boldsymbol{\beta},\mathbf{k}).
\end{aligned} \tag{41}
$$

The computation is therefore reduced to calculating

$$
\Xi_{nn'}^{(0)}(\mathbf{r},\mathbf{k}) \equiv \int_{\mathbf{q}} \frac{e^{i\mathbf{q}\cdot\mathbf{r}}}{q^{2n}|\mathbf{k}+\mathbf{q}|^{2n'}}, \tag{42}
$$

$$
\Xi_{nn'}^{(1)}(\mathbf{r},\mathbf{k}) \equiv \int_{\mathbf{q}} \frac{e^{i\mathbf{q}\cdot\mathbf{r}}}{q^{2n}|\mathbf{k}+\mathbf{q}|^{2n'}} P_{\mathrm{lin}}(q), \tag{43}
$$

which we will discuss below.

B. 2-4 correlations

Similarly, 2-4 correlations with multiple inverse Laplacians of the form

$$I_{24}(k, \boldsymbol{\alpha}, \boldsymbol{\beta}) = \int_{\mathbf{q}_1 \mathbf{q}_2} \frac{e^{i\alpha \cdot \mathbf{q}_1} e^{i\beta \cdot \mathbf{q}_2}}{q_1^{2n_1} |\mathbf{k} + \mathbf{q}_1|^{2n_1'} q_2^{2n_2} |\mathbf{k} + \mathbf{q}_2|^{2n_2'}}$$
$$\times \frac{P_{\lin}(q_1) P_{\lin}(q_2) P_{\lin}(|\mathbf{k} + \mathbf{q}_2|)}{|\mathbf{q}_1 + \mathbf{q}_2|^{2n_3} |\mathbf{k} + \mathbf{q}_1 + \mathbf{q}_2|^{2n_3'}} \quad (44)$$

can be reduced to

$$I_{24}(k, \boldsymbol{\alpha}, \boldsymbol{\beta}) = \int d^3 r e^{i\mathbf{k} \cdot \mathbf{r}} \Xi_{n_3' n_3}^{(0)}(\mathbf{r}, \mathbf{k}) \Xi_{n_1 n_1'}^{(1)}(\mathbf{r} + \boldsymbol{\alpha}, \mathbf{k})$$
$$\times \Xi_{n_2 n_2'}^{(2)}(\mathbf{r} + \boldsymbol{\beta}, \mathbf{k}). \quad (45)$$

Here we defined

$$\Xi_{nn'}^{(2)}(\mathbf{r}, \mathbf{k}) \equiv \int_{\mathbf{q}} \frac{e^{i\mathbf{q} \cdot \mathbf{r}}}{q^{2n} |\mathbf{k} + \mathbf{q}|^{2n'}} P_{\lin}(q) P_{\lin}(|\mathbf{k} + \mathbf{q}|). \quad (46)$$

C. 3-3 correlations

For 3-3 contributions to the power spectrum with multiple inverse Laplacians we consider the general integral

$$I_{33}(k, \boldsymbol{\alpha}, \boldsymbol{\beta}) = \int_{\mathbf{q}_1 \mathbf{q}_2} \frac{e^{i\alpha \cdot \mathbf{q}_1} e^{i\beta \cdot \mathbf{q}_2}}{q_1^{2n_1} |\mathbf{k} + \mathbf{q}_1|^{2n_1'} q_2^{2n_2} |\mathbf{k} + \mathbf{q}_2|^{2n_2'}}$$
$$\times \frac{P_{\lin}(q_1) P_{\lin}(q_2) P_{\lin}(|\mathbf{k} + \mathbf{q}_1 + \mathbf{q}_2|)}{|\mathbf{q}_1 + \mathbf{q}_2|^{2n_3} |\mathbf{k} + \mathbf{q}_1 + \mathbf{q}_2|^{2n_3'}}, \quad (47)$$

which reduces to

$$I_{33}(k, \boldsymbol{\alpha}, \boldsymbol{\beta}) = \int d^3 r e^{i\mathbf{k} \cdot \mathbf{r}} \Xi_{n_3' n_3}^{(1)}(\mathbf{r}, \mathbf{k}) \Xi_{n_1 n_1'}^{(1)}(\mathbf{r} + \boldsymbol{\alpha}, \mathbf{k})$$
$$\times \Xi_{n_2 n_2'}^{(1)}(\mathbf{r} + \boldsymbol{\beta}, \mathbf{k}). \quad (48)$$

D. Evaluating $\Xi^{(n)}$ integrals

It remains to compute the $\Xi^{(n)}$ integrals defined in Eqs. (42), (43) and (46). Similarly to calculations in the rest of the paper (expanding all terms in spherical harmonics or using Eqs. C4, C6 and C7 of [41]) we find

$$\Xi_{nn'}^{(N)}(\mathbf{r}, \mathbf{k}) = \sum_L (-i)^L (2L + 1) \mathsf{P}_L(\hat{\mathbf{r}} \cdot \hat{\mathbf{k}}) Q_{nn',L}^{(N)}(r, k),$$
$$(49)$$

where P_L are Legendre polynomials.

The $Q^{(N)}$ coefficients in Eq. (49) can be computed in two alternative ways. One way is

$$Q_{nn',L}^{(N)}(r, k) = 4\pi \int_0^\infty ds \, s^2 j_L(ks) R_{n'}^{(N)}(s) \int_0^\infty \frac{dq}{2\pi^2}$$
$$\times q^{2-2n} j_L(qs) j_L(qr) \tilde{R}^{(N)}(q), \quad (50)$$

where $\tilde{R}^{(0)}(q) = 1$, $\tilde{R}^{(1,2)}(q) = P_{\lin}(q)$, $R_{n'}^{(0)}(s) = R_{n'}^{(1)}(s) = \Xi_{-2n'}^0(s)$ (see Eq. (G13) and [41]), and $R_{n'}^{(2)}(s) \equiv \xi_{-2n'}^0(s)$. To compute the two-dimensional radial integral in Eq. (50), we need to integrate over q for every value of s and r, and then perform a 1D Hankel transform for every value of r and k to evaluate the integral over s. This procedure is computationally much more expensive than the one-dimensional Hankel transforms in the rest of the paper, but should still be relatively fast compared to the commonly used five-dimensional integrations, noting also that formally related integrals have been successfully computed in another context in [50,68].

An alternative, potentially faster way of computing the $Q^{(N)}$ coefficients in Eq. (49) follows by first expanding $1/|\mathbf{k} + \mathbf{q}|^{2n'}$ in case of $\Xi^{(0)}$ and $\Xi^{(1)}$ or $P_{\lin}(|\mathbf{k} + \mathbf{q}|)/|\mathbf{k} + \mathbf{q}|^{2n'}$ in case of $\Xi^{(2)}$ in Legendre polynomials $\mathsf{P}_L(\hat{\mathbf{k}} \cdot \hat{\mathbf{q}})$. This gives for example

$$Q_{nn',L}^{(2)}(r, k) = \frac{(-1)^L}{(2L + 1)} \int \frac{dq}{2\pi^2} q^{2-2n} j_L(qr) a_{n',L}^{(2)}(k, q)$$
$$\times P_{\lin}(q), \quad (51)$$

where $a_{n',L}^{(2)}(k, q)$ are coefficients in the Legendre expansion above. For $Q^{(1)}$, we obtain the same expression but involving coefficients $a^{(1)}$ that follow from expanding $1/|\mathbf{k} + \mathbf{q}|^{2n'}$. $Q^{(0)}$ can be obtained in the same way by omitting $P_{\lin}(q)$ in Eq. (51).

Finally, the expressions for $\Xi^{(N)}$ from Eq. (49) are collected in the I_n integrals in Eqs. (41), (45) and (48). The result then simplifies by expanding $\exp(i\mathbf{k} \cdot \mathbf{r})$ in Legendre polynomials and using Eq. (G11) for the integral over four Legendre polynomials (assuming the special case $\boldsymbol{\alpha} = \boldsymbol{\beta} = 0$ with trivial numerator).

In Fig. 2 we present the test results for the integrals $I_{15}(k, 0, 0)$, $I_{33}(k, 0, 0)$ and $I_{24}(k, 0, 0)$, with $n_i = n_i' = 1$ and each term in the denominators extended by an infinitesimally small ϵ contribution in order to remove potential singular points, e.g. we have $q^2 \to q^2 + \epsilon$ and similar for the rest of the terms. For realistic P_{15}, P_{33} and P_{24} terms, ϵ can be taken to zero. We compare numerically computed results using Monte Carlo [69] integration (points in Fig. 2) with the results computed with methods presented above using the $\Xi_{nn'}^{(N)}$ functions and Eq. (51) (lines in Fig. 2), finding good overall agreement.

The latter method is computationally much less expensive since we are reducing the five-dimensional integration to 1D integrals (computation of Legendre coefficients $a^{(N)}$) and two sequences of consecutive Hankel transforms
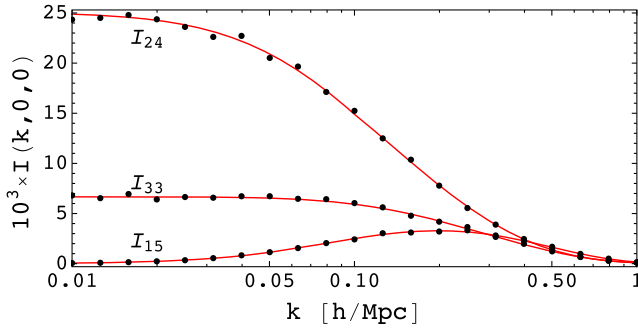
FIG. 2.   Numerical results for two-loop integrals I_{15}, I_{24} and I_{33} defined in Eqs. (40), (44) and (47) for the special case where $\alpha = \beta = 0$ and the linear power spectrum has the simple form $P_{\text{lin}} = k^2 \exp(-k^2)$. Using the radial integrals in Eqs. (41), (45) and (48) together with Eq. (51) (red lines) is compared against the conventionally used direct Monte Carlo evaluation of two-loop integrals using the CUBA [69] library (black points). As mentioned in the text, denominators in the I_{15}, I_{24} and I_{33} terms have been extended, $q^2 \rightarrow q^2 + \epsilon$ with $\epsilon = 0.001$, in order to avoid singular points.

[one to obtain $Q^{(N)}$ using e.g. Eq. (51) and another one to evaluate e.g. Eq. (41)]. Alternatively, $Q^{(N)}$ can be computed using the 2D integration in Eq. (50).

Both methods rely on the (infinite) summation over the multipole number L, but in practice this converges rapidly for $k < 1$ $h\text{Mpc}^{-1}$, so that the summation can be truncated, at least for the simple test case with trivial numerator and exponentially decaying linear power spectrum considered in Fig. 2. Future numerical work is required to check how well this approach works with nontrivial numerators and realistic linear power spectrum.

VI. APPLICABILITY, EXTENSIONS AND DISCUSSION

A. Functional form of the linear input power spectrum

Our equations are formally correct for an arbitrary linear input power spectrum because no step of the derivations makes any assumption about the shape of the input power spectrum. At a practical level, the 1D integrals are 1D Hankel transforms that are nontrivial to evaluate numerically because of highly oscillatory spherical Bessel functions in integrands. Fortunately, these integrals can be evaluated robustly and efficiently as 1D FFTs using the FFTLOG library [62]. This does impose a weak restriction on the shape of the input power spectrum in the sense that it needs to be stored on a discrete 1D grid so that no features finer than the grid resolution can be represented. However, we can use an extremely high resolution for this grid, because we only need to perform one-dimensional FFTs on it, which are extremely fast. This resolution is more than sufficient to resolve features in the power spectrum such as BAO wiggles.

To see this more explicitly, note that the peaks and troughs of the BAO wiggles in the power spectrum have a typical width of $\Delta k \sim 0.02$ $h\text{Mpc}^{-1}$. For our 1D FFTs, we can easily use 10,000 grid points that are logarithmically spaced in 10^{-5} $h\text{Mpc}^{-1} < k < 100$ $h\text{Mpc}^{-1}$. This then gives more than 100 grid points between $k = 0.09$ $h\text{Mpc}^{-1}$ and $k = 0.11$ $h\text{Mpc}^{-1}$, and 40 grid points between $k = 0.29$ $h\text{Mpc}^{-1}$ and $k = 0.31$ $h\text{Mpc}^{-1}$. Every peak and trough of the BAO wiggles can therefore easily be represented with dozens of grid points each, which should indeed be sufficient to accurately model these BAO features.

Another potential restriction is that the FFTs used by FFTLOG may introduce ringing in the Hankel transforms. In [41] we suppressed this by extrapolating the linear input power spectrum with power laws at extremely large scales $k \lesssim 10^{-5}$ $h\text{Mpc}^{-1}$ and at extremely small scales $k \gtrsim 100$ $h\text{Mpc}^{-1}$, which do ultimately not contribute significantly to the power spectrum on scales of practical interest for cosmology. This is therefore just a numerical trick to avoid ringing and should not restrict the applicability of our method in practice (also noting that numerical FFT-PT results for the 1-loop power spectrum were shown to agree with Monte-Carlo integrals at the 10^{-5} level [41]).

B. Number of terms

For 2-loop power spectrum contributions with at most one inverse Laplacian, our final expressions involve only a finite number of terms that need to be summed up. This follows from the fact that the angular structure of the perturbative F_n and G_n kernels does not go beyond a maximum multipole, which in turn follows from the structure of the equations of motion for the DM fluid. Concretely, the F_2 and G_2 kernels involve at most quadrupole terms like $\mathsf{P}_2(\hat{\mathbf{q}}_i \cdot \hat{\mathbf{q}}_j)$, and the recursion relations (A5) imply that in general F_n and G_n involve at most $\mathsf{P}_n(\hat{\mathbf{q}}_i \cdot \hat{\mathbf{q}}_j)$. Therefore, 1-5 terms involve only $\ell \leq 5$, while 2-4 and 3-3 terms involve only $\ell \leq 6$. The total number of terms may still be significant. While we have not checked if this would be an issue in practice, we expect that even a potentially large number of 1D FFTs should be faster than performing five-dimensional Monte-Carlo integrals for every k of interest. The number of FFTs can be reduced by exploiting symmetries to avoid computing the same terms multiple times. Since only a limited number of ξ_n^{ℓ} are needed for all 2-loop integrals, some speedup should also follow by computing all of them with 1D Hankel transforms from a given linear power spectrum and storing them in memory, which is trivial because they are defined on a 1D grid.

For contributions with two or more multiple inverse Laplacians, we followed another approach that involves series of infinitely many terms. For the special cases considered in Section V, we found that they can be

truncated after a few terms. While we expect this to be also the case in full generality, further work is required to check this.

C. Potential infrared divergences

While we showed how to evaluate 2-loop power spectrum contributions using low-dimensional radial integrals, an important future step is to actually implement this and test numerical performance in practice. One potential issue might be that we do not explicitly cancel the sensitivity of individual contributions to very large-scale infrared (IR) modes within integrands [29], but instead we currently rely on accurate cancellations between fully integrated contributions. While this seems problematic for certain power law initial power spectra (scaling universes), it is less problematic for ΛCDM initial power spectra that scale as k^1 on large scales $k \lesssim k_{eq}$. Since the individual contributions should be accurate to machine level precision if evaluated with FFTs, it should be possible to control cancellations of large terms, but this needs to be checked numerically. If this poses problems in practice, an alternative would be to modify the scheme so that IR sensitivity is canceled at an earlier stage of the algorithm. In this context it is also worth noting that our reformulation of 2-loop integrals is by no means unique, and other reformulations may be more suitable for numerical evaluations (also see [41], where vector identities were used to reformulate some 1-loop results).

D. LPT and beyond LCDM

Throughout our paper we have worked with the standard time-independent perturbative F_n kernels in SPT. In LPT, the corresponding kernels have slightly different coefficients but involve the same types of terms when computing cumulants of the displacement field perturbatively (e.g. [15,16,28,70–73]). Our results can therefore straightforwardly be applied to 2-loop integrals if LPT is evaluated order by order, simply by changing coefficients (see [41] for examples of this for 1-loop integrals in LPT). Mapping from the displacement cumulants to the density power spectrum in LPT can involve a second layer of computational complexity, but this can again be reduced to spherical Hankel transforms [38,74].

The form of the perturbative F_n kernels is strictly speaking only valid in an Einstein-de Sitter (EdS) universe. In other cosmologies the kernels can be time-dependent. The effect of this on the 1-loop matter power spectrum is typically at a subpercent level [16,75], but can reach 1% or more when also considering momentum statistics that are relevant for redshift space distortions [58]. It would be interesting to test this approximation at the 2-loop level. While this goes beyond the scope of this paper, our formalism should still apply to the general cosmologies for which Ref. [58] derived separable perturbative kernels.

E. Halo bias

Tracers of the large-scale DM distribution such as halos or galaxies are typically biased with respect to the DM. The relation between halos and DM is often modeled with a bias relation of the form [76,77]

$$\delta_h(\mathbf{x}) = b_1\delta_m(\mathbf{x}) + b_2\delta_m^2(\mathbf{x}) + b_{s2}s_m^2(\mathbf{x}) + b_3\delta_m^3(\mathbf{x}) + \cdots,$$
(52)

where s^2 is the square of the DM tidal tensor, and we did not write down velocity bias and potential other biases. One way to include this in perturbative models is to modify the perturbative F_n kernels such that they relate the nonlinear halo density δ_h to the linear DM density δ_1, i.e.

$$\delta_h(\mathbf{k}) = \tilde{F}_1(\mathbf{k})\delta_1(\mathbf{k})$$
$$+ \int_{\mathbf{q}} \tilde{F}_2(\mathbf{q}, \mathbf{k} - \mathbf{q})\delta_1(\mathbf{q})\delta_1(\mathbf{k} - \mathbf{q}) + \cdots. \quad (53)$$

For example for the above simple bias relation the modified kernels would be $\tilde{F}_1 = b_1$ and

$$\tilde{F}_2(\mathbf{q}, \mathbf{p}) = \left(\frac{17}{21}b_1 + b_2\right) + \frac{b_1}{2}\left(\frac{q}{p} + \frac{p}{q}\right)\hat{\mathbf{q}} \cdot \hat{\mathbf{p}}$$
$$+ \left(\frac{4}{21}b_1 + b_{s^2}\right)\frac{3}{2}\left((\hat{\mathbf{q}} \cdot \hat{\mathbf{p}})^2 - \frac{1}{3}\right). \quad (54)$$

This only changes coefficients, e.g. from $17/21$ to $17/21b_1 + b_2$, without changing the structure of the terms contributing to the kernels. 2-loop corrections to the halo power spectrum can therefore be evaluated in the same way as for the DM power spectrum if the modified coefficients of the halo $\tilde{F}_n$ kernels are used. The G_n velocity kernels should be modified in a similar way.

F. Redshift space distortions

Redshift space distortions (RSD) [78–80] emerge due to the fact that we observe redshifts of galaxies and not directly their positions. The position inferred from the observed redshift is distorted by the peculiar velocity and the comoving redshift-space coordinate for a galaxy is given by

$$\mathbf{s} = \mathbf{x} + \hat{\mathbf{z}}\frac{u_\parallel}{\mathcal{H}} \quad (55)$$

where $\hat{\mathbf{z}}$ is the unit vector along the line of sight, and $u_\parallel$ is the comoving velocity parallel to the line of sight.

There have been several approaches computing the RSD effects within PT [21,81–87]. Even though initial computational routes of these approaches might seem rather different, the results are equivalent, as expected (assuming the

same perturbative order, approximations and resummations in each of the approaches).

In the distribution function (DF) approach [85–89] the overdensity in redshift space is given as the decomposition

$$\delta_s(\mathbf{k}) = \sum_{L=0} \frac{1}{L!} \left(\frac{ik_\parallel}{\mathcal{H}} \right)^L T_\parallel^L(\mathbf{k}), \qquad (56)$$

were $T_\parallel^L(\mathbf{k})$ is the Fourier transform of velocity moments $T_\parallel^L(\mathbf{x}) = (1 + \delta(\mathbf{x}))v_\parallel^L(\mathbf{x})$. It follows that the redshift space power spectrum in the plane-parallel approximation can be written as

$$P^{ss}(\mathbf{k}) = \sum_{\substack{L=0 \\ L'=0}} \frac{(-1)^{L'}}{L!L'!} \left(\frac{ik_\parallel}{\mathcal{H}} \right)^{L+L'} P_{LL'}(\mathbf{k}), \qquad (57)$$

where $P_{LL'}(\mathbf{k}) = \langle T_\parallel^L(\mathbf{k}) | T_\parallel^{*L'}(\mathbf{k}') \rangle'$ are the correlations of the different velocity moments. Using rotational symmetry, as shown in [85,86], each of the $P_{LL'}$ spectra can be further decomposed in the form

$$P_{LL'}(\mathbf{k}) = \sum_{\substack{l=L,L-2,\dots \\ l'=L',L'-2,\dots \\ m=0\dots l}} P_{l,l'}^{L,L',m}(k) \mathsf{P}_l^m(\mu) \mathsf{P}_{l'}^m(\mu), \qquad (58)$$

where $\mathsf{P}_l^m(\mu)$ are the associated Legendre polynomials, and $\mu = \hat{\mathbf{z}} \cdot \hat{\mathbf{k}}$. It is important to note that the decomposed spectra $P_{l,l'}^{L,L',m}$ depend only on the magnitude k of the wave vector $\mathbf{k}$. Also note that the decomposition above gives a finite number of terms for each L and L'. Explicit PT expression for all the 1-loop $P_{l,l'}^{L,L',m}$ contributions are given in Ref. [86]. They can be constructed from $I_{nm}(k)$ and $J_{nm}(k)$ expressions given in Appendix D of Ref. [86]. It is clear that the FFT-PT method used for the fast computation of the P_{22} and P_{13} 1-loop contributions from Ref. [41] is straightforwardly applicable to the integrals $I_{nm}(k)$ (convolution type integrals similar to P_{22}) and $J_{nm}(k)$ (propagator type integrals similar to P_{13}).

It is important to note that the decomposition of the RSD effect into the $P_{l,l'}^{L,L',m}(k)$ spectra does not rely on PT and is valid up to all orders. So analogous expressions as presented up to one loop in [86] can be computed up to two loop. For these correlations the methods presented in this paper would be fully applicable.

As mentioned, an advantage of the DF approach lies in the use of rotational symmetries to determine the angular structure of RSD correlators valid regardless of the PT order. One-loop RSD power spectrum results obtained in some of the other references [21,81–83,90] reduce after explicit calculation to the same angular structure, as expected, finally reaching the same conclusion, albeit, in a less transparent way. Our treatment of RSD corrections to the 2-loop power spectrum is therefore not restricted to the DF approach but applies to all the other RSD modeling

approaches mentioned above. This discussion should also be valid at higher orders.

Similar conclusions (keeping in mind Sec. VI E) hold for biased tracers in redshift space where the explicit decompositions using the DF approach can be found in [87]. From the above it follows that equivalent conclusions hold also for velocity statistics (pairwise velocity and pairwise dispersion) in real and redshift space and the explicit DF decomposition presented in [91].

As mentioned above, our methods for rapid loop computations can also be performed in LPT (for explicit 1-loop expressions see appendices in e.g. [15]). For LPT models of RSD effects in addition to the biasing effects see e.g. [92,93].

VII. CONCLUSIONS

Pushing models of the large-scale structure of the universe to nonlinear scales is a challenging problem in cosmology. An extensively studied approach to this is perturbation theory. Unfortunately, perturbative corrections come in the form of high-dimensional loop integrals that are cumbersome to evaluate. For example, the 2-loop power spectrum involves five-dimensional integrals at every wave number of interest.

Generalizing previous work on the 1-loop matter power spectrum [41,42], we show in this paper how 2-loop corrections to the density power spectrum in Eulerian standard perturbation theory can be rewritten so that they involve only low-dimensional radial integrals. In absence of multiple inverse Laplacians, these take the form of one-dimensional Hankel transforms that can be evaluated very efficiently with one-dimensional FFTs using FFTLOG [62]. Contributions arising from multiple inverse Laplacians seem to require a sequence of low-dimensional radial integrals, which are computationally more challenging but may still be faster than five-dimensional integrations (see Sec. V).

One specific application of the method is the possibility to speed up Monte-Carlo chains when fitting cosmological parameters from LSS observations. More generally, the fast expressions can be useful for anyone working with the 2-loop power spectrum or higher-order loop integrals in general.

Our reformulation of 2-loop power spectrum integrals is based on avoiding convolution integrals by repeatedly changing between Fourier and position space, integrating over orientations, and performing the remaining radial integrals using one-dimensional FFTs. This is very general in the sense that it does not assume a specific shape for the linear input power spectrum. This, in turn, is important to accurately model the imprint of baryonic acoustic oscillations on LSS 2-point statistics, which is arguably the most pristine cosmological signal measured with high precision from modern surveys.

The result that three-dimensional loop integrals can be reduced to one-dimensional radial integrals is not a

coincidence, but can be understood from the fact that structure formation only depends on distances between objects if we assume statistical isotropy and homogeneity and the standard fluid equations of motion with their standard perturbative solution (also see [41]).

We show how the same method can be applied to the 2-loop power spectrum of halos or any other biased tracer of the dark matter with known bias relation. Redshift space distortions can also be handled with this method. This is straightforward to see for the distribution function approach to model redshift space distortions but also applies to many other RSD modeling approaches (see Sec. VI F). Our method should also apply to Lagrangian space models as shown for the 1-loop case in [41]. For the special, presumably only academically interesting case of scaling universes with perfect power law initial power spectrum, the one-dimensional FFTs can be evaluated analytically so that all 2-loop power spectrum contributions reduce to simple power laws (see Appendix F).

In the future, it would be interesting to numerically implement the fast 2-loop expressions presented in our paper, extending the 1-loop implementations of [41,42]. It would also be useful to include effective field theory corrections and generalize the method to higher-order statistics like the bispectrum or trispectrum. These possible directions of future investigation seem worthwhile pursuing given the impressive amount of upcoming data from a number of planned LSS surveys in the near future and the need to analyze and model these observations beyond the linear regime to maximize their science returns.

ACKNOWLEDGMENTS

APPENDIX A: PERTURBATIVE EXPANSION AND GRAVITY KERNELS

This section provides a brief overview of the perturbative approach to solve the equations of motion in Eulerian standard perturbation theory (see [16] for a review).

We start form the standard ansatz for the expansion of density and velocity divergence field

$$\delta(\mathbf{k}, \tau) = \sum_{n=0}^{\infty} \delta^{(n)}(\mathbf{k}, \tau), \tag{A1}$$

$$\theta(\mathbf{k}, \tau) = -f(\tau)\mathcal{H}(\tau) \sum_{n=0}^{\infty} \theta^{(n)}(\mathbf{k}, \tau), \tag{A2}$$

where we have for a given order

$$\delta^{(n)}(\mathbf{k}, \tau) = \int_{\mathbf{q}_1 \ldots \mathbf{q}_n} (2\pi)^3 \delta^D(\mathbf{k} - \mathbf{q}_1 \ldots - \mathbf{q}_n)$$
$$\times F_n^{(s)}(\mathbf{q}_1, \ldots, \mathbf{q}_n)\delta_1(\mathbf{q}_1, \tau)\ldots\delta_1(\mathbf{q}_n, \tau),$$

$$\theta^{(n)}(\mathbf{k}, \tau) = \int_{\mathbf{q}_1 \ldots \mathbf{q}_n} (2\pi)^3 \delta^D(\mathbf{k} - \mathbf{q}_1 \ldots - \mathbf{q}_n)$$
$$\times G_n^{(s)}(\mathbf{q}_1, \ldots, \mathbf{q}_n)\delta_1(\mathbf{q}_1, \tau)\ldots\delta_1(\mathbf{q}_n, \tau). \tag{A3}$$

By definition the first order kernels are unity, i.e. $F_1^{(s)} = G_1^{(s)} = 1$. Since the linear solution δ_1 is known, all higher order nonlinearities are incorporated in the kernels $F_n^{(s)}$ and $G_n^{(s)}$. The upper index (s) denotes symmetrized kernels,

$$F_n^{(s)}(\mathbf{q}_1, \ldots, \mathbf{q}_n) = \frac{1}{n!} \sum_\pi F_n(\pi\{\mathbf{q}_1, \ldots, \mathbf{q}_n\}),$$

$$G_n^{(s)}(\mathbf{q}_1, \ldots, \mathbf{q}_n) = \frac{1}{n!} \sum_\pi G_n(\pi\{\mathbf{q}_1, \ldots, \mathbf{q}_n\}). \tag{A4}$$

Unsymmetrized kernels satisfy recursion relations that can be derived by substituting Eq. (A3) into the equations of motion Eq. (11). These recursion relations are

$$F_n(\mathbf{q}_1, \ldots, \mathbf{q}_n) = \sum_{m=1}^{n-1} \frac{G_m(\mathbf{q}_1, \ldots, \mathbf{q}_m)}{(2n+3)(n-1)}$$
$$\times \left\{ (2n+1) \frac{\mathbf{k} \cdot \mathbf{q}_{1\cdots m}}{q_{1\cdots m}^2} F_{n-m}(\mathbf{q}_{m+1}, \ldots, \mathbf{q}_n) \right.$$
$$\left. + \frac{k^2 \mathbf{q}_{1\cdots m} \cdot \mathbf{q}_{m+1\cdots n}}{q_{1\cdots m}^2 q_{m+1\cdots n}^2} G_{n-m}(\mathbf{q}_{m+1}, \ldots, \mathbf{q}_n) \right\} \tag{A5}$$

and

$$G_n(\mathbf{q}_1, \ldots, \mathbf{q}_n) = \sum_{m=1}^{n-1} \frac{G_m(\mathbf{q}_1, \ldots, \mathbf{q}_m)}{(2n+3)(n-1)}$$
$$\times \left\{ 3 \frac{\mathbf{k} \cdot \mathbf{q}_{1\cdots m}}{q_{1\cdots m}^2} F_{n-m}(\mathbf{q}_{m+1}, \ldots, \mathbf{q}_n) \right.$$
$$+ n \frac{k^2 \mathbf{q}_{1\cdots m} \cdot \mathbf{q}_{m+1\cdots n}}{q_{1\cdots m}^2 q_{m+1\cdots n}^2}$$
$$\left. \times G_{n-m}(\mathbf{q}_{m+1}, \ldots, \mathbf{q}_n) \right\} \tag{A6}$$

where we have introduced the notation $\mathbf{q}_{1\cdots m} = \mathbf{q}_1 + \cdots + \mathbf{q}_m$ and $\mathbf{q}_{m+1\cdots n} = \mathbf{q}_{m+1} + \cdots + \mathbf{q}_n$. Also $\mathbf{k} = \mathbf{q}_1 + \cdots + \mathbf{q}_n$ in the last two equations.

APPENDIX B: COUPLING FACTORS

This Appendix provides analytical expressions for the coupling factors $\mathcal{M}_n$ that arise from the angular structure of

2-loop integrands and are used throughout the paper. The first few examples are evaluated in Table I.

1-5 correlations without inverse Laplacians in Eq. (18) are proportional to the coupling factor $\mathcal{M}_0$ defined by

$$\mathcal{M}_0(\ell_0, \ell_1, \ell_2) \equiv \sum_{\ell'=0}^{\min(\ell_0, \ell_1, \ell_2)} \alpha_{\ell_0\ell'}\alpha_{\ell_1\ell'}\alpha_{\ell_2\ell'}(2\ell'+1).$$

(B1)

The $\alpha_{\ell\ell'}$ coefficients follow from decomposing products between wave vectors in spherical harmonics using Eq. (G3), and are given by [36,41]

$$\alpha_{\ell\ell'} = \frac{1}{2}\int_{-1}^{1}d\mu\,\mu^{\ell}\mathsf{P}_{\ell'}(\mu)$$

$$= \begin{cases} \frac{\ell!}{2^{(\ell-\ell')/2}[(\ell-\ell')/2]!(\ell+\ell'+1)!!}, & \text{if } \ell \geq \ell' \,\&\, \ell+\ell' \text{ even,} \\ 0, & \text{otherwise.} \end{cases}$$

(B2)

These coefficients vanish if the second index ℓ' is greater than the first index ℓ, which helps to render sums in the paper finite. They are normalized so that $\alpha_{00} = 1$. The $\mathcal{M}_0$ coupling factor in Eq. (B1) is symmetric in its arguments, and all nonzero factors for $l_i \leq 2$ are listed in Table I.

The coupling factor $\mathcal{M}_1$ between (ℓ_1, ℓ_2, ℓ_3) and L that enters in Eq. (21) is defined as

$$\mathcal{M}_1(\ell_1, \ell_2, \ell_3; L)$$

$$\equiv (-1)^L(2L+1)\sum_{\ell_1'=0}^{\ell_1}\alpha_{\ell_1\ell_1'}(2\ell_1'+1)$$

$$\times \sum_{\ell'=0}^{\min(\ell_2,\ell_3)}\alpha_{\ell_2\ell'}\alpha_{\ell_3\ell'}(2\ell'+1)\begin{pmatrix} L & \ell_1' & \ell' \\ 0 & 0 & 0 \end{pmatrix}^2.$$

(B3)

This involves a Wigner 3-j symbol, which imposes a triangle condition that implies $L \leq \ell_1' + \ell' \leq \ell_1 + \min(\ell_2, \ell_3)$. The range of allowed L in Eq. (21) is therefore finite. The coupling factor is symmetric under $\ell_2 \leftrightarrow \ell_3$. For $\ell_i \leq 1$ the only nonzero couplings are shown in Table I.

In Eq. (C8) we used the coupling factor $\mathcal{M}_2$ between (ℓ_1, ℓ_2, ℓ_3) and (L, L'), which is defined as

$$\mathcal{M}_2(\ell_1, \ell_2, \ell_3; L, L')$$

$$\equiv (-1)^{L+L'}(2L+1)(2L'+1)\sum_{\ell_1'=0}^{\ell_1}\sum_{\ell_2'=0}^{\ell_2}\sum_{\ell_3'=0}^{\ell_3}\alpha_{\ell_1\ell_1'}\alpha_{\ell_2\ell_2'}\alpha_{\ell_3\ell_3'}$$

$$\times (2\ell_1'+1)(2\ell_2'+1)(2\ell_3'+1)\begin{pmatrix} \ell_1' & L' & \ell_2' \\ 0 & 0 & 0 \end{pmatrix}^2$$

$$\times \begin{pmatrix} \ell_2' & L & \ell_3' \\ 0 & 0 & 0 \end{pmatrix}^2.$$

(B4)

The 3-j symbols impose triangle conditions on (L', ℓ_1', ℓ_2') and (L, ℓ_2', ℓ_3'), which make the sums over L and L' in Eq. (C8) finite. The coupling factor is symmetric under simultaneously changing $\ell_1 \leftrightarrow \ell_3$ and $L \leftrightarrow L'$. All nonzero couplings for $\ell_1 \leq \ell_2 \leq \ell_3 \leq 1$ are listed in Table I.

Finally, several expressions involve the coupling $\mathcal{M}_3$ between (ℓ_1, ℓ_2, ℓ_3) and (L_1, L_2, L_3) defined by

$$\mathcal{M}_3(\ell_1, \ell_2, \ell_3; L_1, L_2, L_3)$$

$$\equiv \sum_{\ell_1'=0}^{\ell_1}\sum_{\ell_2'=0}^{\ell_2}\sum_{\ell_3'=0}^{\ell_3}\alpha_{\ell_1\ell_1'}\alpha_{\ell_2\ell_2'}\alpha_{\ell_3\ell_3'}\begin{Bmatrix} L_1 & L_2 & L_3 \\ \ell_1' & \ell_2' & \ell_3' \end{Bmatrix}'.$$

(B5)

This involves a rescaled 6-j symbol defined in Eq. (G14). It severely restricts the allowed values for L_i so that e.g. the sum on the right-hand side of Eq. (24) is finite. [94].

APPENDIX C: 2-4 CORRELATIONS WITH INVERSE LAPLACIANS AND NONTRIVIAL ANGULAR DEPENDENCE

This Appendix shows how to evaluate nontrivial 2-4 correlations with inverse Laplacians and nontrivial angular dependence, providing details of the results summarized in Sec. IV B 2. Additional details on the derivation of these results will be provided in Appendix D.

1. Most general form of 2-4 correlations

As mentioned before, the loop correction to the SPT power spectrum generated by 2-4 correlations is

$$P_{24}(k) = 24\int_{\mathbf{q}_1\mathbf{q}_2}F_4^{(s)}(\mathbf{q}_1, -\mathbf{q}_1, \mathbf{q}_2, \mathbf{k}-\mathbf{q}_2)F_2^{(s)}(\mathbf{q}_2, \mathbf{k}-\mathbf{q}_2)$$

$$\times P_{\text{lin}}(q_1)P_{\text{lin}}(q_2)P_{\text{lin}}(|\mathbf{k}-\mathbf{q}_2|).$$

(C1)

The most general form of terms contributing to this is

$$\int_{\mathbf{q}_1\mathbf{q}_2}[\hat{\mathbf{q}}_2\cdot(\widehat{\mathbf{k}-\mathbf{q}_2})]^{\ell_1}[\hat{\mathbf{q}}_1\cdot(\widehat{\mathbf{k}-\mathbf{q}_2})]^{\ell_2}(\hat{\mathbf{q}}_1\cdot\hat{\mathbf{q}}_2)^{\ell_3}$$

$$\times \frac{q_1^{n_1}P_{\text{lin}}(q_1)q_2^{n_2}P_{\text{lin}}(q_2)|\mathbf{k}-\mathbf{q}_2|^{n_3}P_{\text{lin}}(|\mathbf{k}-\mathbf{q}_2|)}{|s_1\mathbf{q}_1 + s_2\mathbf{q}_2 + s_3(\mathbf{k}-\mathbf{q}_2)|^2},$$

(C2)

where the momenta entering the denominator or inverse Laplacian are parametrized by the parameters $s_1 \in \{-1, 0, 1\}$ and s_2, $s_3 \in \{0, 1\}$. The only cases not already covered by Eq. (21) occur when at least two of these s_i parameters are nonzero. The angular structure in Eq. (C2) is sufficiently general because it accounts for all scalar products that can be formed between the arguments of F_4 and between the arguments of F_2 in Eq. (C1).

2. Splitting in two nested 1-loop integrals

We now show how to evaluate the most general form of 2-4 correlations given in Eq. (C2) by splitting it into two nested 1-loop integrals as demonstrated for a simpler case in Eq. (33). We proceed in two steps: First, we calculate the loop integral over the $\mathbf{q}_1$ momentum that connects the F_4 vertex to itself, corresponding to the red tadpole subdiagram in Fig. 1. We then insert the result and compute the integral over the other loop momentum $\mathbf{q}_2$ that connects the F_4 and F_2 vertices, corresponding to the blue subdiagram in Fig. 1.

Explicitly, to evaluate the 2-loop integral of Eq. (C2), we write scalar products involving the tadpole momentum $\mathbf{q}_1$ in terms of spherical harmonics, e.g.

$$(\hat{\mathbf{q}}_1 \cdot \hat{\mathbf{q}}_2)^{\ell_3} = 4\pi \sum_{\boldsymbol{\ell}_3'}^{\ell_3} \alpha_{\ell_3 \ell_3'} Y_{\boldsymbol{\ell}_3'}(\hat{\mathbf{q}}_1) Y_{\boldsymbol{\ell}_3'}^*(\hat{\mathbf{q}}_2), \quad \text{(C3)}$$

where we use the condensed notation $\boldsymbol{\ell} = (\ell, m)$ and $\sum_{\boldsymbol{\ell}'} = \sum_{\ell'=0}^{\ell} \sum_{m'=-\ell'}^{\ell'}$. Generalizing Eq. (31), the integral (C2) then splits into an outer $\mathbf{q}_2$-integral

$$\int_{\mathbf{q}_2 \mathbf{q}_1} [\hat{\mathbf{q}}_2 \cdot (\widehat{\mathbf{k} - \mathbf{q}_2})]^{\ell_1} [\hat{\mathbf{q}}_1 \cdot (\widehat{\mathbf{k} - \mathbf{q}_2})]^{\ell_2} (\hat{\mathbf{q}}_1 \cdot \hat{\mathbf{q}}_2)^{\ell_3}$$

$$\times \frac{q_1^{n_1} P_{\text{lin}}(q_1) q_2^{n_2} P_{\text{lin}}(q_2) |\mathbf{k} - \mathbf{q}_2|^{n_3} P_{\text{lin}}(|\mathbf{k} - \mathbf{q}_2|)}{|s_1 \mathbf{q}_1 + s_2 \mathbf{q}_2 + s_3 (\mathbf{k} - \mathbf{q}_2)|^2}$$

$$= 4\pi \int_{\mathbf{q}_2} [\hat{\mathbf{q}}_2 \cdot (\widehat{\mathbf{k} - \mathbf{q}_2})]^{\ell_1} q_2^{n_2} P_{\text{lin}}(q_2) |\mathbf{k} - \mathbf{q}_2|^{n_3}$$

$$\times P_{\text{lin}}(|\mathbf{k} - \mathbf{q}_2|) \sum_{\boldsymbol{\ell}_2'}^{\ell_2} \sum_{\boldsymbol{\ell}_3'}^{\ell_3} \alpha_{\ell_2 \ell_2'} Y_{\boldsymbol{\ell}_2'}^*(\widehat{\mathbf{k} - \mathbf{q}_2})$$

$$\times P_{\text{tadpole}}^{\boldsymbol{\ell}_2' \boldsymbol{\ell}_3' s_1 n_1}(s_2 \mathbf{q}_2 + s_3(\mathbf{k} - \mathbf{q}_2)) \alpha_{\ell_3 \ell_3'} Y_{\boldsymbol{\ell}_3'}^*(\hat{\mathbf{q}}_2), \quad \text{(C4)}$$

over an inner tadpole integral over $\mathbf{q}_1$,

$$P_{\text{tadpole}}^{\boldsymbol{\ell}_2' \boldsymbol{\ell}_3' s_1 n_1}(\mathbf{p}) \equiv 4\pi \int_{\mathbf{q}_1} Y_{\boldsymbol{\ell}_2'}(\hat{\mathbf{q}}_1) Y_{\boldsymbol{\ell}_3'}(\hat{\mathbf{q}}_1) \frac{q_1^{n_1} P_{\text{lin}}(q_1)}{|s_1 \mathbf{q}_1 + \mathbf{p}|^2}, \quad \text{(C5)}$$

which is evaluated at the momentum $\mathbf{p} \equiv s_2 \mathbf{q}_2 + s_3(\mathbf{k} - \mathbf{q}_2)$. Splitting the 2-loop integral in these two nested 1-loop integrals is the main trick needed for evaluating P_{24}.

The remaining procedure to evaluate the outer and inner tadpole 1-loop integrals in Eqs. (C4) and (C5) is similar to Sec. IV B 1 and [41], as we show next.

3. Evaluating the tadpole 1-loop integral over $\mathbf{q}_1$

The only cases for the denominator in Eq. (C2) that are not already covered by the separable case in Eq. (21) are $(s_1, s_2, s_3) \in \{(\pm 1, 1, 0), (\pm 1, 0, 1), (\pm 1, 1, 1)\}$, corresponding to $\mathbf{p} \in \{\mathbf{q}_2, \mathbf{k} - \mathbf{q}_2, \mathbf{k}\}$ and $s_1 = \pm 1$. We therefore only consider these cases in the following. The different cases correspond to different couplings and fields on which the inverse Laplacian acts, generalizing Eq. (30) from Sec. IV B 1.

In each case, the inner tadpole integral (C5) is a Fourier-space convolution that reduces to a position space product of $\Xi_{-2}^0(r) = (4\pi r)^{-1}$ defined in Eq. (G13) and the correlation $\xi_{n_1, s_1}^L(r)$ defined in Eq. (29):

$$P_{\text{tadpole}}^{\boldsymbol{\ell}_2' \boldsymbol{\ell}_3' s_1 n_1}(\mathbf{p}) = 4\pi \sum_{L=0}^{\infty} \sum_{M=-L}^{L} (-1)^L \mathcal{G}_{\boldsymbol{\ell}_2' \boldsymbol{\ell}_3' \mathbf{L}} Y_{\mathbf{L}}^*(\hat{\mathbf{p}}) \mathcal{P}_{n_1, s_1}^L(p)$$

(C6)

with

$$\mathcal{P}_{n_1, s_1}^L(p) \equiv \int_0^{\infty} dr \, r j_L(pr) \xi_{n_1, s_1}^L(r). \quad \text{(C7)}$$

This follows by integrating over orientations of the tadpole momentum $\mathbf{q}_1$ and expanding in multipoles of the momentum $\mathbf{p}$. For $\ell_2' = \ell_3' = n_1 = 0$, $s_1 = 1$ and $\mathbf{p} = \mathbf{q}_2$, we recover the simpler result of Eq. (32) because $\mathcal{G}_{000} = Y_0^*(\hat{\mathbf{p}}) = (4\pi)^{-1/2}$.

To proceed with the evaluation of the outer integral over $\mathbf{q}_2$ in Eq. (C4), we consider the cases $\mathbf{p} \in \{\mathbf{q}_2, \mathbf{k} - \mathbf{q}_2, \mathbf{k}\}$ separately.

4. Evaluating the outer 1-loop integral: Case 1

We start with the case $\mathbf{p} = \mathbf{q}_2$ in Eq. (C5), i.e. $(s_1, s_2, s_3) = (\pm 1, 1, 0)$. As shown in detail in Appendix D, using Eq. (C6) in Eq. (C4), performing angular integrations, and exploiting orthogonality relations of Wigner 3-j symbols leads to

$$\int \frac{d\Omega_{\hat{\mathbf{k}}}}{4\pi} \int_{\mathbf{q}_1 \mathbf{q}_2} [\hat{\mathbf{q}}_2 \cdot (\widehat{\mathbf{k} - \mathbf{q}_2})]^{\ell_1} [\hat{\mathbf{q}}_1 \cdot (\widehat{\mathbf{k} - \mathbf{q}_2})]^{\ell_2} (\hat{\mathbf{q}}_1 \cdot \hat{\mathbf{q}}_2)^{\ell_3} \frac{q_1^{n_1} P_{\text{lin}}(q_1) q_2^{n_2} P_{\text{lin}}(q_2) |\mathbf{k} - \mathbf{q}_2|^{n_3} P_{\text{lin}}(|\mathbf{k} - \mathbf{q}_2|)}{|s_1 \mathbf{q}_1 + \mathbf{q}_2|^2}$$

$$= 4\pi \int_0^{\infty} dr \, r^2 j_0(kr) \sum_{L=0}^{\ell_2 + \ell_3} \sum_{L'=0}^{\ell_1 + \ell_2} \mathcal{M}_2(\ell_1, \ell_2, \ell_3; L, L') \mathcal{T}_{LL'}^{s_1 n_1 n_2}(r) \xi_{n_3}^{L'}(r).$$

(C8)

This is a 1D Hankel transform of a sum of position space products of 4-point like correlations $\mathcal{T}(r)$ and linear correlation functions $\xi(r)$. The former is a generalization of Eq. (34), given by a 1D Hankel transform of the Fourier space product of the linear power spectrum and the transformed linear correlation function $\mathcal{P}$ from Eq. (C7):

$$T_{LL'}^{s_1 n_1 n_2}(r) = \int_0^\infty \frac{dq_2}{2\pi^2} q_2^{n_2+2} j_{L'}(q_2 r) P_{\text{lin}}(q_2) \mathcal{P}_{n_1,s_1}^L(q_2). \tag{C9}$$

The coupling factor $\mathcal{M}_2$ is defined by Eq. (B4). In the simple special case $\ell_1 = \ell_2 = \ell_3 = 0$, the only nonvanishing coupling is $\mathcal{M}_2(0,0,0;0,0) = 1$, so that the general result of Eq. (C8) simplifies and we recover the simple result of Eq. (33) derived earlier (for $s_1 = 1$).

The case $\mathbf{p} = \mathbf{k} - \mathbf{q}_2$ in Eq. (C5) with $(s_1, s_2, s_3) = (\pm 1, 0, 1)$ follows by symmetry, noting that the result

above does not change if we change the integration variable from $\mathbf{q}_2$ to $\mathbf{k} - \mathbf{q}_2$. Indeed, if we change the denominator on the left-hand side of Eq. (C8) to $|s_1 \mathbf{q}_1 + \mathbf{k} - \mathbf{q}_2|^{-2}$, the right-hand side follows by relabeling $\ell_2 \leftrightarrow \ell_3$ and $n_2 \leftrightarrow n_3$.

5. Evaluating the outer 1-loop integral: Case 2

The last case is $\mathbf{p} = \mathbf{k}$ in Eq. (C5), i.e. $(s_2, s_3) = (1,1)$. This case is related to the following contraction of the inverse Laplacian acting on a cubic field:

$$\int d^3 r\, e^{i\mathbf{k}\cdot\mathbf{r}} \langle \overline{\delta_1(\mathbf{x})\delta_1(\mathbf{x})}\, \overline{\delta_1(\mathbf{x}')\nabla^{-2}[\delta_1(\mathbf{x}')\delta_1(\mathbf{x}')\delta_1(\mathbf{x}')]} \rangle = -\int_{\mathbf{q}_1 \mathbf{q}_2} \frac{P_{\text{lin}}(q_1) P_{\text{lin}}(\mathbf{q}_2) P_{\text{lin}}(\mathbf{k} - \mathbf{q}_2)}{|\mathbf{q}_1 + \mathbf{k}|^2}. \tag{C10}$$

The fully general case additionally contains scalar products between wave vectors. It can be reduced to (see endnote [95])

$$\int \frac{d\Omega_{\hat{\mathbf{k}}}}{4\pi} \int_{\mathbf{q}_1 \mathbf{q}_2} [\hat{\mathbf{q}}_2 \cdot \widehat{(\mathbf{k} - \mathbf{q}_2)}]^{\ell_1} [\hat{\mathbf{q}}_1 \cdot \widehat{(\mathbf{k} - \mathbf{q}_2)}]^{\ell_2} (\hat{\mathbf{q}}_1 \cdot \hat{\mathbf{q}}_2)^{\ell_3} \frac{q_1^{n_1} P_{\text{lin}}(q_1) q_2^{n_2} P_{\text{lin}}(q_2) |\mathbf{k} - \mathbf{q}_2|^{n_3} P_{\text{lin}}(|\mathbf{k} - \mathbf{q}_2|)}{|s_1 \mathbf{q}_1 + \mathbf{k}|^2}$$

$$= 4\pi \sum_{L=0}^{\ell_2+\ell_3} \mathcal{P}_{n_1,s_1}^L(k) \int_0^\infty dr\, r^2 j_L(kr) \sum_{L_2=0}^{\ell_1+\ell_3} \sum_{L_3=0}^{\ell_1+\ell_2} \mathcal{M}_3(\ell_1, \ell_2, \ell_3; L, L_2, L_3) \xi_{n_2}^{L_2}(r) \xi_{n_3}^{L_3}(r). \tag{C11}$$

This involves the Hankel transform of a sum of products of two correlation functions, multiplied by the power spectrum-like quantity $\mathcal{P}(k)$ from Eq. (C7). The coupling factor $\mathcal{M}_3$ from Eq. (B5) enforces triangle conditions for (L, ℓ_2', ℓ_3'), (L_2, ℓ_1', ℓ_3'), (L_3, ℓ_1', ℓ_2') and (L, L_2, L_3), restricting the sums over L, L_2 and L_3 in Eq. (C11) to be finite.

APPENDIX D: DERIVATION OF 2-4 CORRELATIONS WITH INVERSE LAPLACIAN AND NONTRIVIAL ANGULAR DEPENDENCE

In this section we provide details for the derivation of Eq. (C8), which is a fast expression for contributions to P_{24} that contain an inverse Laplacian with $\mathbf{p} = \mathbf{q}_2$ in Eq. (C4). We explicitly show the steps for this particular case, noting that most other calculations in this paper proceed similarly in flavor but are typically less involved.

Introducing the auxiliary variable $\mathbf{q}_3 = \mathbf{k} - \mathbf{q}_2$ with a Dirac delta on the right-hand side of Eq. (C4) and using Eq. (C6) for the tadpole integral evaluated at $\mathbf{p} = \mathbf{q}_2$ gives

$$P_{24,\text{nonsep}}^{\ell_1 \ell_2 \ell_3 \mathbf{n} s_1}(k) \equiv \int \frac{d\Omega_{\hat{\mathbf{k}}}}{4\pi} \int_{\mathbf{q}_1 \mathbf{q}_2} [\hat{\mathbf{q}}_2 \cdot \widehat{(\mathbf{k} - \mathbf{q}_2)}]^{\ell_1} [\hat{\mathbf{q}}_1 \cdot \widehat{(\mathbf{k} - \mathbf{q}_2)}]^{\ell_2} (\hat{\mathbf{q}}_1 \cdot \hat{\mathbf{q}}_2)^{\ell_3} \frac{q_1^{n_1} P_{\text{lin}}(q_1) q_2^{n_2} P_{\text{lin}}(q_2) |\mathbf{k} - \mathbf{q}_2|^{n_3} P_{\text{lin}}(|\mathbf{k} - \mathbf{q}_2|)}{|s_1 \mathbf{q}_1 + \mathbf{q}_2|^2}$$

$$= (4\pi)^2 \int \frac{d\Omega_{\hat{\mathbf{k}}}}{4\pi} \int_{\mathbf{q}_2 \mathbf{q}_3} \int d^3 r\, e^{i\mathbf{r}\cdot(\mathbf{q}_3 - \mathbf{k} + \mathbf{q}_2)} (\hat{\mathbf{q}}_2 \cdot \hat{\mathbf{q}}_3)^{\ell_1} q_2^{n_2} P_{\text{lin}}(q_2) q_3^{n_3} P_{\text{lin}}(q_3)$$

$$\times \sum_{\ell_2'}^{\ell_2} \sum_{\ell_3'}^{\ell_3} \sum_{\mathbf{L}}^{\ell_2+\ell_3} \alpha_{\ell_2 \ell_2'} Y_{\ell_2'}^*(\hat{\mathbf{q}}_3)(-1)^L \mathcal{G}_{\ell_2' \mathbf{L} \ell_3'} Y_{\mathbf{L}}^*(\hat{\mathbf{q}}_2) \mathcal{P}_{n_1,s_1}^L(q_2) \alpha_{\ell_3 \ell_3'} Y_{\ell_3'}^*(\hat{\mathbf{q}}_2). \tag{D1}$$

The angular integrals over $\hat{\mathbf{k}}$ and $\hat{\mathbf{r}}$ can be performed by noting that Eq. (G2) implies

$$\int \frac{d\Omega_{\hat{\mathbf{k}}}}{4\pi} \int d\Omega_{\hat{\mathbf{r}}}\, e^{i\mathbf{r}\cdot(\mathbf{q}_3 - \mathbf{k} + \mathbf{q}_2)} = (4\pi)^2 j_0(kr) \sum_{\mathbf{L}'}^\infty (-1)^{L'} j_{L'}(q_2 r) j_{L'}(q_3 r) Y_{\mathbf{L}'}(\hat{\mathbf{q}}_2) Y_{\mathbf{L}'}^*(\hat{\mathbf{q}}_3). \tag{D2}$$

This gives

$$P_{24,\text{nonsep}}^{\ell_1\ell_2\ell_3\mathbf{n}s_1}(k) = (4\pi)^5 \int_0^\infty dr\, r^2 j_0(kr) \int_{\mathbf{q}_2\mathbf{q}_3} \sum_{\ell_1'}^{\ell_1} \alpha_{\ell_1\ell_1'} Y_{\ell_1'}(\hat{\mathbf{q}}_2) Y_{\ell_1'}^*(\hat{\mathbf{q}}_3) q_2^{n_2} P_{\text{lin}}(q_2) q_3^{n_3} P_{\text{lin}}(q_3)$$

$$\times \sum_{\mathbf{L}'}^\infty (-1)^{L'} j_{L'}(q_2 r) j_{L'}(q_3 r) Y_{\mathbf{L}'}(\hat{\mathbf{q}}_2) Y_{\mathbf{L}'}^*(\hat{\mathbf{q}}_3)$$

$$\times \sum_{\ell_2'}^{\ell_2} \sum_{\ell_3'}^{\ell_3} \sum_{\mathbf{L}}^{\ell_2+\ell_3} \alpha_{\ell_2\ell_2'} Y_{\ell_2'}^*(\hat{\mathbf{q}}_3)(-1)^L \mathcal{G}_{\ell_2'\mathbf{L}\ell_3'} Y_{\mathbf{L}}^*(\hat{\mathbf{q}}_2) \mathcal{P}_{n_1,s_1}^L(q_2)\alpha_{\ell_3\ell_3'} Y_{\ell_3'}^*(\hat{\mathbf{q}}_2), \tag{D3}$$

where we also expressed $(\hat{\mathbf{q}}_2 \cdot \hat{\mathbf{q}}_3)^{\ell_1}$ in the first line in terms of spherical harmonics using Eq. (G3). The integral over $\hat{\mathbf{q}}_3$ is a Gaunt integral (G4), giving $\mathcal{G}_{\ell_1'\mathbf{L}'\ell_2'}$. The integral over $\hat{\mathbf{q}}_2$ follows from Eq. (G7), giving $\sum_{\mathbf{L}''}\mathcal{G}_{\ell_1'\mathbf{L}'\mathbf{L}''}\mathcal{G}_{\mathbf{L}''\mathbf{L}\ell_3'}$. Using an orthogonality relation for Wigner 3-j symbols, Eq. (G8), the sums over m_1' and M' simplify to

$$\sum_{m_1'M'}\mathcal{G}_{\ell_1'\mathbf{L}'\ell_2'}\mathcal{G}_{\ell_1'\mathbf{L}'\mathbf{L}''} = \frac{1}{2l_2'+1}\delta_{\ell_2'L''}\delta_{m_2'M''}(\mathcal{H}_{\ell_1'L'\ell_2'})^2. \tag{D4}$$

The same applies to the sum over M and m_3':

$$\sum_{Mm_3'}\mathcal{G}_{\ell_2'\mathbf{L}\ell_3'}\mathcal{G}_{\mathbf{L}''\mathbf{L}\ell_3'} = \frac{1}{2l_2'+1}\delta_{\ell_2'L''}\delta_{m_2'M''}(\mathcal{H}_{\ell_2'L\ell_3'})^2. \tag{D5}$$

The sum over m_2' then gives $2l_2' + 1$. The $\mathcal{H}$ factors defined in Eq. (G5) contain 3-j symbols that restrict the sums over L and L' to be finite. The integral over q_3 gives $\xi_{n_3}^{L'}(r)$. We thus arrive at

$$P_{24,\text{nonsep}}^{\ell_1\ell_2\ell_3\mathbf{n}s_1}(k) = 4\pi \int_0^\infty dr\, r^2 j_0(kr) \sum_{L=0}^{\ell_2+\ell_3} \sum_{L'=0}^{\ell_1+\ell_2} \xi_{n_3}^{L'}(r) \int \frac{dq_2}{2\pi^2} q_2^{2+n_2} j_{L'}(q_2 r) P_{\text{lin}}(q_2)\mathcal{P}_{n_1,s_1}^L(q_2)$$

$$\times (-1)^{L+L'} \sum_{\ell_1'=0}^{\ell_1} \sum_{\ell_2'=0}^{\ell_2} \sum_{\ell_3'=0}^{\ell_3} \alpha_{\ell_1\ell_1'}\alpha_{\ell_2\ell_2'}\alpha_{\ell_3\ell_3'} \frac{(4\pi)^2}{2\ell_2'+1} (\mathcal{H}_{\ell_1'L'\ell_2'}\mathcal{H}_{\ell_2'L\ell_3'})^2. \tag{D6}$$

This agrees with Eq. (C8) above.

APPENDIX E: DERIVATION OF 3-3 CORRELATIONS WITH INVERSE LAPLACIAN

1. Simple example

In this section we derive Eq. (36), which is a simple example of a 3-3 correlation with inverse Laplacian.

Introducing $\mathbf{q}_3 \equiv \mathbf{k} - \mathbf{q}_1 - \mathbf{q}_2$ with a Dirac delta on the left-hand side of Eq. (36), decomposing it in plane waves, and performing the integral over $\mathbf{q}_3$ gives

$$\int \frac{d\Omega_{\hat{\mathbf{k}}}}{4\pi} \int_{\mathbf{q}_1\mathbf{q}_2} \frac{P_{\text{lin}}(q_1)P_{\text{lin}}(q_2)P_{\text{lin}}(|\mathbf{k}-\mathbf{q}_1-\mathbf{q}_2|)}{|\mathbf{q}_1+\mathbf{q}_2|^2}$$

$$= \int \frac{d\Omega_{\hat{\mathbf{k}}}}{4\pi} \int d^3\mathbf{r}\, e^{-i\mathbf{k}\cdot\mathbf{r}} \xi_0^0(r)\mathbb{T}(r), \tag{E1}$$

where we defined the 4-point like quantity $\mathbb{T}(r)$ by

$$\mathbb{T}(r) \equiv \int_{\mathbf{q}_1\mathbf{q}_2} \frac{P_{\text{lin}}(q_1)P_{\text{lin}}(q_2)}{|\mathbf{q}_1+\mathbf{q}_2|^2} e^{i\mathbf{q}_1\cdot\mathbf{r}} e^{i\mathbf{q}_2\cdot\mathbf{r}}. \tag{E2}$$

To simplify $\mathbb{T}(r)$, we introduce $\mathbf{q}_4 \equiv \mathbf{q}_1 + \mathbf{q}_2$ with a Dirac delta and perform the integrals over $\mathbf{q}_1$ and $\mathbf{q}_2$ to get

$$\mathbb{T}(r) = \int_{\mathbf{q}_4} \int d^3\mathbf{r}' \frac{\xi_0^0(|\mathbf{r}-\mathbf{r}'|)\xi_0^0(|\mathbf{r}-\mathbf{r}'|)}{q_4^2} e^{i\mathbf{q}_4\cdot\mathbf{r}'}. \tag{E3}$$

The integral over $\mathbf{r}'$ has the form of a convolution. To solve this, we introduce $\mathbf{r}'' \equiv \mathbf{r} - \mathbf{r}'$ with a Dirac delta, decompose this in plane waves, and integrate over $\mathbf{r}'$ to get (this is equivalent to changing integration variables $\mathbf{r}' \to \mathbf{r} - \mathbf{r}'$)

$$\mathbb{T}(r) = \int_{\mathbf{q}_4} e^{i\mathbf{q}_4\cdot\mathbf{r}} \int d^3\mathbf{r}'' \frac{\xi_0^0(r'')\xi_0^0(r'')}{q_4^2} e^{-i\mathbf{q}_4\cdot\mathbf{r}''}. \tag{E4}$$

Using Eq. (G12), the integral over $\hat{\mathbf{r}}''$ gives $4\pi j_0(q_4 r'')$. Then, the integral over $\hat{\mathbf{q}}_4$ gives $4\pi j_0(q_4 r)$. We are thus left with

$$\mathbb{T}(r) = \int_0^\infty \frac{\mathrm{d}q_4}{2\pi^2} j_0(q_4 r) \int_0^\infty \mathrm{d}r''(r'')^2 j_0(q_4 r'') \xi_0^0(r'') \xi_0^0(r''),$$
(E5)

which agrees with Eq. (37) in the main text.

As an aside, we note that an alternative simplification of $\mathbb{T}(r)$ follows by first integrating over $\mathbf{q}_4$ in Eq. (E3),

$$\mathbb{T}(r) = \int \mathrm{d}^3\mathbf{r}' \frac{\xi_0^0(|\mathbf{r}-\mathbf{r}'|)\xi_0^0(|\mathbf{r}-\mathbf{r}'|)}{4\pi r'},$$
(E6)

but this 3D convolution integral does not seem suitable for fast numerical evaluation.

2. General case

In this section we derive the right-hand side of Eq. (38), which allows for fast evaluation of general 3-3 correlations with inverse Laplacian and nontrivial angular structure in the integrand. The derivation proceeds similarly to the simpler example above, the only addition being the nontrivial angular structure of the integrand, which is taken care of by expansions in spherical harmonics.

In detail, Eq. (38) can be derived as follows. Introducing $\mathbf{q}_4 \equiv \mathbf{q}_1 + \mathbf{q}_2$ with a second Dirac delta on the left-hand side of Eq. (38) and expanding both Dirac deltas in plane waves yields

$$P_{33,\mathrm{nonsep}}^{\ell_1\ell_2\ell_3,\mathbf{n}}(k) \equiv k^{n_0} \int \frac{\mathrm{d}\Omega_{\hat{\mathbf{k}}}}{4\pi} \int_{\mathbf{q}_1\mathbf{q}_2\mathbf{q}_3} (2\pi)^3 \delta_D(\mathbf{k} - \mathbf{q}_1 - \mathbf{q}_2 - \mathbf{q}_3) \frac{(\hat{\mathbf{q}}_1\cdot\hat{\mathbf{q}}_2)^{\ell_3}(\hat{\mathbf{q}}_2\cdot\hat{\mathbf{q}}_3)^{\ell_1}(\hat{\mathbf{q}}_1\cdot\hat{\mathbf{q}}_3)^{\ell_2}}{|\mathbf{q}_1+\mathbf{q}_2|^{n_4}} \prod_{i=1}^3 q_i^{n_i} P_{\mathrm{lin}}(q_i) \quad (E7)$$

$$= \int \frac{\mathrm{d}\Omega_{\hat{\mathbf{k}}}}{4\pi} \int \mathrm{d}^3\mathbf{r} \int \mathrm{d}^3\mathbf{r}' e^{-i\mathbf{k}\cdot\mathbf{r}} \int_{\mathbf{q}_1\cdots\mathbf{q}_4} e^{i\mathbf{q}_4\cdot\mathbf{r}'} e^{i\mathbf{q}_1\cdot(\mathbf{r}-\mathbf{r}')} e^{i\mathbf{q}_2\cdot(\mathbf{r}-\mathbf{r}')} e^{i\mathbf{q}_3\cdot\mathbf{r}} \frac{k^{n_0}}{q_4^{n_4}} (\hat{\mathbf{q}}_1\cdot\hat{\mathbf{q}}_2)^{\ell_3}(\hat{\mathbf{q}}_2\cdot\hat{\mathbf{q}}_3)^{\ell_1}(\hat{\mathbf{q}}_1\cdot\hat{\mathbf{q}}_3)^{\ell_2} \prod_{i=1}^3 q_i^{n_i} P_{\mathrm{lin}}(q_i).$$
(E8)

Introducing $\mathbf{r}'' \equiv \mathbf{r} - \mathbf{r}'$ with another Dirac delta and expanding it in plane waves gives

$$P_{33,\mathrm{nonsep}}^{\ell_1\ell_2\ell_3,\mathbf{n}}(k) = \int \frac{\mathrm{d}\Omega_{\hat{\mathbf{k}}}}{4\pi} \int \mathrm{d}^3\mathbf{r} \int \mathrm{d}^3\mathbf{r}' \int \mathrm{d}^3\mathbf{r}'' \int_{\mathbf{q}} \int_{\mathbf{q}_1\cdots\mathbf{q}_4} e^{i\mathbf{q}\cdot(\mathbf{r}''-\mathbf{r}+\mathbf{r}')} e^{-i\mathbf{k}\cdot\mathbf{r}} e^{i\mathbf{q}_4\cdot\mathbf{r}'} e^{i\mathbf{q}_1\cdot\mathbf{r}''} e^{i\mathbf{q}_2\cdot\mathbf{r}''} e^{i\mathbf{q}_3\cdot\mathbf{r}}$$

$$\times \frac{k^{n_0}}{q_4^{n_4}} (\hat{\mathbf{q}}_1\cdot\hat{\mathbf{q}}_2)^{\ell_3}(\hat{\mathbf{q}}_2\cdot\hat{\mathbf{q}}_3)^{\ell_1}(\hat{\mathbf{q}}_1\cdot\hat{\mathbf{q}}_3)^{\ell_2} \prod_{i=1}^3 q_i^{n_i} P_{\mathrm{lin}}(q_i).$$
(E9)

Using Eq. (G12), the integral over $\hat{\mathbf{k}}$ gives $j_0(kr)$, and the integral over $\hat{\mathbf{q}}_4$ gives $4\pi j_0(q_4 r')$. Then, the integral over $\hat{\mathbf{r}}'$ yields $4\pi j_0(qr')$. Next we expand the remaining plane waves and the scalar products between wave vectors in spherical harmonics [using Eq. (G3) for the latter]. This leads to two spherical harmonics with argument $\hat{\mathbf{q}}$, so that the integral over $\hat{\mathbf{q}}$ gives a Kronecker delta. The same happens for the integral over $\hat{\mathbf{r}}$. Additionally, there are three spherical harmonics with argument $\hat{\mathbf{q}}_1$, so that integrating over $\hat{\mathbf{q}}_1$ gives a Gaunt integral (G4). The same happens for integrals over $\hat{\mathbf{q}}_2$, $\hat{\mathbf{q}}_3$ and $\hat{\mathbf{r}}''$. The integral over r' follows from the closure relation for spherical Bessel functions, enforcing $q_4 = q$, and yielding the intermediate result

$$P_{33,\mathrm{nonsep}}^{\ell_1\ell_2\ell_3,\mathbf{n}}(k) = k^{n_0} \frac{(4\pi)^{10}}{[(2\pi)^3]^5} \frac{\pi}{2} \int_0^\infty \mathrm{d}r\,\mathrm{d}r'' \mathrm{d}q\,\mathrm{d}q_1 \mathrm{d}q_2 \mathrm{d}q_3\, r^2 (r'')^2 q^{2-n_4} \left[\prod_{i=1}^3 q_i^{2+n_i} P_{\mathrm{lin}}(q_i) \right]$$

$$\times \sum_{L_{1,2,3}\ell'_{1,2,3}} i^{L_1+L_2+L_3} (-1)^{\ell'_1+\ell'_2+\ell'_3} \alpha_{\ell_1\ell'_1}\alpha_{\ell_2\ell'_2}\alpha_{\ell_3\ell'_3} j_0(kr) j_{L_3}(qr) j_{L_3}(qr'') j_{L_1}(q_1 r'') j_{L_2}(q_2 r'') j_{L_3}(q_3 r)$$

$$\times \sum_{M_{1,2,3}m'_{1,2,3}} (-1)^{m'_1+m'_2+m'_3} \mathcal{G}_{L_1\ell'_2\ell'_3}^{M_1 m'_2 m'_3} \mathcal{G}_{L_2\ell'_1\ell'_3}^{M_2 m'_1 -m'_3} \mathcal{G}_{L_3\ell'_1\ell'_2}^{M_3 -m'_1 -m'_2} \mathcal{G}_{L_1 L_2 L_3}^{M_1 M_2 M_3}.$$
(E10)

The last sum of four Gaunt integrals over M_i and m'_i gives a 6-j symbol (G14). Conveniently arranging the integration order then allows to write the P_{33} integral as a sum over 1D Hankel transforms as in Eq. (38) in the main text.

Some comments regarding the derivation are in order. In this section we only consider a quadratic denominator,

$n_4 = 2$, corresponding to a single inverse Laplacian, but the calculation above formally works for any n_4, which is why we gave the result for arbitrary n_4 (noting though that some integrals may diverge for $n_4 \neq 2$). In the special case without denominator, $n_4 = 0$, the integral over q in Eq. (39) yields a Dirac delta enforcing $r = r''$, so that

we recover Eq. (24). As an alternative way to simplify the integral on the left-hand side of Eq. (38) one could split the derivative with respect to **r** into radial and angular parts, similarly to e.g. [53]. This is convenient for $n_4 = 2$ but gets likely more complicated for larger n_4, whereas the results above apply to general n_4.

APPENDIX F: SPECIALIZATION TO SCALING UNIVERSE WITH PERFECT POWER LAW INITIAL POWER SPECTRUM

The DM power spectrum in a ΛCDM cosmology is scale-dependent and includes features like baryonic acoustic oscillations. Therefore, integrals over this power spectrum or Hankel transforms must be performed *numerically*, e.g. using FFTLog [62]. This is the primary use case we envision for our method, because it allows evaluating 2-loop corrections to the matter power spectrum in an extremely fast way for arbitrary shapes of the initial linear power spectrum. In this section we specialize the general results from the rest of the paper to a simpler special case in which the transforms can actually be performed *analytically*, exploiting the fact that the Hankel transform of a power law is again a power law. This may be useful for validating numerical implementations, but we stress again that it is not needed for our method which applies to arbitrary linear power spectrum shapes.

For scaling universes the DM power spectrum is assumed to have a power-law shape,

$$P_{\text{lin}}(k) = \left(\frac{k}{k_0}\right)^N, \qquad (F1)$$

with some slope N and pivot scale k_0. The linear correlation function ξ_n^ℓ then reduces to

$$[\xi_n^l(r)]_{\text{scal.uni.}} = \frac{1}{k_0^N} \int_0^\infty \frac{dq}{2\pi^2} q^{2+n+N} j_l(qr)$$

$$= \frac{\Xi_{n+N}^l(r)}{k_0^N}, \qquad (F2)$$

where the integral over q is a Hankel transform of a power law. This is again a power law

$$\Xi_{n+N}^l(r) = \frac{2^{n+N}}{\pi\sqrt{\pi}} \frac{\Gamma(\frac{l+n+N+3}{2})}{\Gamma(\frac{l-n-N}{2})} \frac{1}{r^{3+n+N}} \qquad (F3)$$

if $n + N < -1$, $n + N + l > -3$ and $r > 0$ [41,96–98]. In the rest of this section we use this result to specialize the fast expressions in the main text of the paper to scaling universes, obtaining analytical solutions for all 2-loop integrals in scaling universes.

1. 1-5 correlations in a scaling universe

For example, in a scaling universe, the fast expression for 1-5 correlations given by the right-hand side of

Eq. (28) reduces to a simple power law in k (assuming $s_0 = s_1 = s_2 = 1$)

$$[\text{Eq. (28)}]_{\text{scal.uni.}} = c_{15} \frac{k^{n_0+N}}{k_0^N} k^{4+2N+n_1+n_2}, \qquad (F4)$$

where the proportionality constant is

$$c_{15} = \frac{\sqrt{\pi}}{(4\pi)^3 (k_0)^{2N}} \sum_{L_0=0}^{\ell_1+\ell_2} \frac{\Gamma(\frac{L_0-4-2N-n_1-n_2}{2})}{\Gamma(\frac{L_0+7+2N+n_1+n_2}{2})}$$

$$\times \sum_{L_1=0}^{\ell_0+\ell_1} \sum_{L_2=0}^{\ell_0+\ell_2} \mathcal{M}_3(\ell_0, \ell_1, \ell_2; L_0, L_2, L_1)$$

$$\times \prod_{i=1}^2 \frac{\Gamma(\frac{L_i+n_i+N+3}{2})}{\Gamma(\frac{L_i-n_i-N}{2})}. \qquad (F5)$$

For $N = -2.6$ and $\ell_i = n_i = 0$, we validated Eq. (F4) numerically by brute-force integrating the left-hand side using the Monte-Carlo integration library CUBA [69].

2. 2-4 correlations in a scaling universe

We can also simplify the fully general 2-4 correlations of Eq. (C8) in a perfectly scaling universe. To see this, note that the transformed correlation $\mathcal{P}(p)$ of Eq. (C7) becomes a power law in a scaling universe,

$$[\mathcal{P}_{n_1,1}^L(p)]_{\text{scal.uni.}} = \frac{1}{8\pi k_0^N} \frac{\Gamma(\frac{L+n_1+N+3}{2})}{\Gamma(\frac{L-n_1-N}{2})}$$

$$\times \frac{\Gamma(\frac{L-n_1-N-1}{2})}{\Gamma(\frac{L+n_1+N+4}{2})} p^{1+n_1+N}. \qquad (F6)$$

Then the 4-point-like correlation $\mathcal{T}(r)$ in Eq. (C9) also becomes a power law,

$$[\mathcal{T}_{LL'}^{1,n_1 n_2}(r)]_{\text{scal.uni.}} = \frac{2^{1+n_1+n_2+2N}[\mathcal{P}_{n_1,1}^L(1)]_{\text{scal.uni.}}}{\pi\sqrt{\pi} k_0^N r^{4+n_1+n_2+2N}}$$

$$\times \frac{\Gamma(\frac{L'+n_1+n_2+2N+4}{2})}{\Gamma(\frac{L'-n_1-n_2-2N-1}{2})}. \qquad (F7)$$

Therefore the right-hand side of the 2-4 integral in Eq. (C8) also turns into a simple power law in k (assuming $s_1 = 1$),

$$[\text{Eq.(C8)}]_{\text{scal.uni.}} = c_{24} k^{4+n_1+n_2+n_3+3N} \qquad (F8)$$

with proportionality constant

$$c_{24} = \frac{1}{2^{6+n_1+n_2+2N}k_0^N} \frac{\Gamma(\frac{-4-n_1-n_2-n_3-3N}{2})}{\Gamma(\frac{7+n_1+n_2+n_3+3N}{2})}$$

$$\times \sum_{L=0}^{\ell_2+\ell_3} \sum_{L'=0}^{\ell_1+\ell_2} \mathcal{M}_2(\ell_1,\ell_2,\ell_3;L,L')$$

$$\times [\mathcal{T}_{LL'}^{1,n_1 n_2}(1)]_{\text{scal.uni.}} \frac{\Gamma(\frac{L'+n_3+N+3}{2})}{\Gamma(\frac{L'-n_3-N}{2})}. \qquad (\text{F9})$$

The other case of general 2-4 correlations is given by Eq. (C11). This takes the same power law form in a scaling universe (assuming again $s_1 = 1$)

$$[\text{Eq.(C11)}]_{\text{scal.uni.}} = c_{24}' k^{4+n_1+n_2+n_3+3N} \qquad (\text{F10})$$

but the proportionality constant is now

$$c_{24}' = \sum_{L=0}^{\ell_2+\ell_3} \frac{[\mathcal{P}_{n_1,1}^L(1)]_{\text{scal.uni.}}}{8\pi\sqrt{\pi}k_0^{2N}} \frac{\Gamma(\frac{L-n_2-n_3-2N-3}{2})}{\Gamma(\frac{L+n_2+n_3+2N+6}{2})}$$

$$\times \sum_{L_2=0}^{\ell_1+\ell_3} \sum_{L_3=0}^{\ell_1+\ell_2} \mathcal{M}_3(\ell_1,\ell_2,\ell_3;L,L_2,L_3)$$

$$\times \frac{\Gamma(\frac{L_2+n_2+N+3}{2})}{\Gamma(\frac{L_2-n_2-N}{2})} \frac{\Gamma(\frac{L_3+n_3+N+3}{2})}{\Gamma(\frac{L_3-n_3-N}{2})}. \qquad (\text{F11})$$

For $N = -2.6$ and $n_i = \ell_i = 0$, Eqs. (F8) and (F10) are consistent with results obtained by Monte-Carlo integrating the left-hand side.

3. 3-3 correlations in a scaling universe

The fast expression for 3-3 correlations without inverse Laplacians given by the right-hand side of Eq. (24) also reduce to a simple power law in k for scaling universes,

$$[\text{Eq. (24)}]_{\text{scal.uni.}} = c_{33} k^{6+n_1+n_2+n_3+3N}, \qquad (\text{F12})$$

where the proportionality constant is

$$c_{33} = \frac{1}{(4\pi)^3 (k_0)^{3N}} \frac{\Gamma(\frac{-n_1-n_2-n_3-3N-6}{2})}{\Gamma(\frac{n_1+n_2+n_3+3N+9}{2})}$$

$$\times \sum_{L_1=0}^{\ell_2+\ell_3} \sum_{L_2=0}^{\ell_1+\ell_3} \sum_{L_3=0}^{\ell_1+\ell_2} \mathcal{M}_3(\ell_1,\ell_2,\ell_3;L_1,L_2,L_3)$$

$$\times \prod_{i=1}^{3} \frac{\Gamma(\frac{L_i+n_i+N+3}{2})}{\Gamma(\frac{L_i-n_i-N}{2})}. \qquad (\text{F13})$$

We numerically validated this both for scaling universes and for a realistic linear input power spectrum for $\ell_i = n_i = 0$.

More general 3-3 correlations with inverse Laplacians are given in Eq. (38). For a scaling universe, the 4-point

like-quantity $\mathcal{T}(r)$ from Eq. (39) becomes a power law,

$$[\mathbb{T}_{L_3}^{\ell_1\ell_2\ell_3,n_1n_2n_4}(r)]_{\text{scal.uni.}}$$

$$= \frac{2^{n_1+n_2-n_4+2N-2}}{\pi^4 k_0^{2N} r^{n_1+n_2-n_4+2N+6}}$$

$$\times \frac{\Gamma(\frac{L_3+n_1+n_2-n_4+2N+6}{2})}{\Gamma(\frac{L_3-n_1-n_2+n_4-2N-3}{2})} \frac{\Gamma(\frac{L_3-n_1-n_2-2N-3}{2})}{\Gamma(\frac{L_3+n_1+n_2+2N+6}{2})}$$

$$\times \sum_{L_1=|\ell_2-\ell_3|}^{\ell_2+\ell_3} \sum_{L_2=|\ell_1-\ell_3|}^{\ell_1+\ell_3} \mathcal{M}_3(\ell_1,\ell_2,\ell_3;L_1,L_2,L_3)$$

$$\times \frac{\Gamma(\frac{L_1+n_1+N+3}{2})}{\Gamma(\frac{L_1-n_1-N}{2})} \frac{\Gamma(\frac{L_2+n_2+N+3}{2})}{\Gamma(\frac{L_2-n_2-N}{2})}. \qquad (\text{F14})$$

The right-hand side of Eq. (38) therefore becomes

$$[\text{Eq. (38)}]_{\text{scal.uni.}} = c_{33}' k^{6+n_1+n_2+n_3-n_4+3N}, \qquad (\text{F15})$$

with proportionality constant

$$c_{33}' = \frac{1}{(2\pi)^3 (k_0)^{3N}} \frac{\Gamma(\frac{-n_1-n_2-n_3+n_4-3N-6}{2})}{\Gamma(\frac{n_1+n_2+n_3-n_4+3N+9}{2})}$$

$$\times \sum_{L_3=|\ell_1-\ell_2|}^{\ell_1+\ell_2} \frac{\Gamma(\frac{L_3+n_1+n_2-n_4+2N+6}{2})}{\Gamma(\frac{L_3-n_1-n_2+n_4-2N-3}{2})} \frac{\Gamma(\frac{L_3-n_1-n_2-2N-3}{2})}{\Gamma(\frac{L_3+n_1+n_2+2N+6}{2})}$$

$$\times \sum_{L_1=|\ell_2-\ell_3|}^{\ell_2+\ell_3} \sum_{L_2=|\ell_1-\ell_3|}^{\ell_1+\ell_3} \mathcal{M}_3(\ell_1,\ell_2,\ell_3;L_1,L_2,L_3)$$

$$\times \prod_{i=1}^{3} \frac{\Gamma(\frac{L_i+n_i+N+3}{2})}{\Gamma(\frac{L_i-n_i-N}{2})}. \qquad (\text{F16})$$

Numerically validating this result is unfortunately not straightforward because the brute force integration of the left-hand side seems nontrivial for scaling universes. Nevertheless, the predicted scaling with k does seem consistent with brute force integration if we choose $N = -2.1$.

APPENDIX G: USEFUL MATHEMATICAL IDENTITIES

For convenience we list some standard mathematical identities that we used throughout this paper (also see Appendix C in [41]).

1. Expansions

Some of the most frequently used relations in our paper are the expansion of a Dirac delta in plane waves,

$$(2\pi)^3 \delta_D(\mathbf{q}) = \int d^3\mathbf{r} e^{i\mathbf{q}\cdot\mathbf{r}}, \qquad (\text{G1})$$

the expansion of plane waves in spherical harmonics,

$$e^{\pm ia\mathbf{k}\cdot\mathbf{r}} = 4\pi \sum_{l=0}^{\infty} \sum_{m=-l}^{l} (\pm i\,\mathrm{sgn}(a))^l j_l(|a|kr) Y_{lm}(\hat{\mathbf{k}}) Y_{lm}^*(\hat{\mathbf{r}}),$$

(G2)

and the decomposition of scalar products between wave vectors into spherical harmonics,

$$(\hat{\mathbf{x}} \cdot \hat{\mathbf{y}})^\ell = 4\pi \sum_{\ell'=0}^{\ell} \sum_{m'=-\ell'}^{\ell'} \alpha_{\ell\ell'} Y_{\ell'm'}(\hat{\mathbf{x}}) Y_{\ell'm'}^*(\hat{\mathbf{y}}),$$

(G3)

where $\alpha_{\ell\ell'}$ coefficients are given by Eq. (B2).

2. Angular integrals and Wigner 3-j symbols

The integral over three spherical harmonics is a Gaunt integral that contains Wigner 3-j symbols,

$$\int d\Omega_{\hat{\mathbf{q}}} Y_{\ell_1}(\hat{\mathbf{q}}) Y_{\ell_2}(\hat{\mathbf{q}}) Y_{\ell_3}(\hat{\mathbf{q}}) = \mathcal{G}_{\ell_1\ell_2\ell_3}$$

$$= \mathcal{H}_{\ell_1\ell_2\ell_3} \begin{pmatrix} \ell_1 & \ell_2 & \ell_3 \\ m_1 & m_2 & m_3 \end{pmatrix},$$

(G4)

where the isotropic part is

$$\mathcal{H}_{\ell_1\ell_2\ell_3} \equiv \sqrt{\frac{(2\ell_1+1)(2\ell_2+1)(2\ell_3+1)}{4\pi}} \begin{pmatrix} \ell_1 & \ell_2 & \ell_3 \\ 0 & 0 & 0 \end{pmatrix}.$$

(G5)

The indices must satisfy $m_1 + m_2 + m_3 = 0$, $|\ell_2 - \ell_3| \le \ell_1 \le \ell_2 + \ell_3$ and permutations, and $\ell_1 + \ell_2 + \ell_3$ must be even. The Gaunt coefficients (G4) represent the coefficients that arise when decomposing the product of two spherical harmonics in terms of a third one, i.e.

$$Y_{\ell_1}(\hat{\mathbf{q}}) Y_{\ell_2}(\hat{\mathbf{q}}) = \sum_{L=|\ell_1-\ell_2|}^{\ell_1+\ell_2} \sum_{M=-L}^{L} \mathcal{G}_{\ell_1\ell_2 L} Y_L^*(\hat{\mathbf{q}}).$$

(G6)

The integral over four spherical harmonics is therefore

$$\int d\Omega_{\hat{\mathbf{q}}} Y_{\ell_1}(\hat{\mathbf{q}}) Y_{\ell_2}(\hat{\mathbf{q}}) Y_{\ell_3}^*(\hat{\mathbf{q}}) Y_{\ell_4}^*(\hat{\mathbf{q}}) = \sum_L \mathcal{G}_{\ell_1\ell_2 L} \mathcal{G}_{L\ell_3\ell_4}.$$

(G7)

The Wigner 3-j symbols satisfy the following orthogonality relation:

$$\sum_{m_1 m_2} \begin{pmatrix} \ell_1 & \ell_2 & \ell \\ m_1 & m_2 & m \end{pmatrix} \begin{pmatrix} \ell_1 & \ell_2 & \ell' \\ m_1 & m_2 & m' \end{pmatrix} = \frac{1}{2\ell+1} \delta_{\ell\ell'} \delta_{mm'}.$$

(G8)

Some other relations used in our paper are

$$\sum_m (-1)^m \begin{pmatrix} \ell & \ell & L \\ m & -m & 0 \end{pmatrix} = (-1)^\ell \sqrt{2\ell+1}\, \delta_{L0} \quad \text{(G9)}$$

and

$$\begin{pmatrix} \ell & \ell & 0 \\ m & -m & 0 \end{pmatrix} = \frac{(-1)^{\ell-m}}{\sqrt{2\ell+1}}.$$

(G10)

Equations (G6)–(G10) can be used to perform the angular integral over the product of four Legendre polynomials with the same argument

$$\int d\Omega_{\hat{\mathbf{r}}} P_{\ell_1}(\hat{\mathbf{k}} \cdot \hat{\mathbf{r}}) P_{\ell_2}(\hat{\mathbf{k}} \cdot \hat{\mathbf{r}}) P_{\ell_3}(\hat{\mathbf{k}} \cdot \hat{\mathbf{r}}) P_{\ell_4}(\hat{\mathbf{k}} \cdot \hat{\mathbf{r}})$$

$$= 4\pi \sum_L (2L+1) \begin{pmatrix} L & \ell_1 & \ell_2 \\ 0 & 0 & 0 \end{pmatrix}^2 \begin{pmatrix} L & \ell_3 & \ell_4 \\ 0 & 0 & 0 \end{pmatrix}^2,$$

(G11)

where the sum over L is restricted by triangle conditions.

The angular part of the 3D Fourier transform of a function $f(r)$ that depends only on radius is

$$\int d\Omega_{\hat{\mathbf{q}}} e^{\pm i\mathbf{q}\cdot\mathbf{r}} f(r) = 4\pi j_0(qr) f(r).$$

(G12)

The Fourier transform of the inverse Laplacian is (e.g. [41])

$$\Xi_{-2}^0(r) \equiv \int_{\mathbf{q}} e^{-i\mathbf{q}\cdot\mathbf{r}} \frac{1}{q^2} = \int_0^\infty \frac{dq}{2\pi^2} j_0(qr) = \frac{1}{4\pi r}.$$

(G13)

3. Wigner 6-j symbol

We sometimes use a rescaled 6-j symbol defined by

$$\begin{Bmatrix} j_1 & j_2 & j_3 \\ j_4 & j_5 & j_6 \end{Bmatrix}'$$

$$\equiv (4\pi)^2 i^{j_1+j_2+j_3} (-1)^{j_4+j_5+j_6} \mathcal{H}_{j_1 j_2 j_3}$$

$$\times \mathcal{H}_{j_1 j_5 j_6} \mathcal{H}_{j_2 j_4 j_6} \mathcal{H}_{j_3 j_4 j_5} \begin{Bmatrix} j_1 & j_2 & j_3 \\ j_4 & j_5 & j_6 \end{Bmatrix}$$

$$= i^{j_1+j_2+j_3} (-1)^{j_4+j_5+j_6} \begin{pmatrix} j_1 & j_2 & j_3 \\ 0 & 0 & 0 \end{pmatrix} \begin{pmatrix} j_1 & j_5 & j_6 \\ 0 & 0 & 0 \end{pmatrix}$$

$$\times \begin{pmatrix} j_2 & j_4 & j_6 \\ 0 & 0 & 0 \end{pmatrix} \begin{pmatrix} j_3 & j_4 & j_5 \\ 0 & 0 & 0 \end{pmatrix} \begin{Bmatrix} j_1 & j_2 & j_3 \\ j_4 & j_5 & j_6 \end{Bmatrix}$$

$$\times \prod_{i=1}^{6} (2j_i + 1).$$

(G14)

This is only nonzero if triangle conditions of the form $|j_2 - j_3| \leq j_1 \leq j_2 + j_3$ are satisfied for (j_1, j_2, j_3), (j_1, j_5, j_6), (j_2, j_4, j_6) and (j_3, j_4, j_5). Additionally, $j_1 + j_2 + j_3$, $j_1 + j_5 + j_6$, $j_2 + j_4 + j_6$ and $j_3 + j_4 + j_5$ must be even. The product of the first 3-j symbol and the 6-j symbol in Eq. (G14) can also be replaced by a sum over 3-j symbols using Eq. 34.5.23 of [96,97]:

$$
\begin{Bmatrix} j_1 & j_2 & j_3 \\ j_4 & j_5 & j_6 \end{Bmatrix}' = i^{j_1+j_2+j_3} \begin{pmatrix} j_1 & j_5 & j_6 \\ 0 & 0 & 0 \end{pmatrix} \begin{pmatrix} j_2 & j_4 & j_6 \\ 0 & 0 & 0 \end{pmatrix}
$$

$$
\times \begin{pmatrix} j_3 & j_4 & j_5 \\ 0 & 0 & 0 \end{pmatrix} \left[\prod_{n=1}^{6} (2j_n + 1) \right] \sum_{m=-\max(j_4,j_5,j_6)}^{\max(j_4,j_5,j_6)} (-1)^m
$$

$$
\times \begin{pmatrix} j_1 & j_5 & j_6 \\ 0 & m & -m \end{pmatrix} \begin{pmatrix} j_2 & j_4 & j_6 \\ 0 & m & -m \end{pmatrix} \begin{pmatrix} j_3 & j_4 & j_5 \\ 0 & m & -m \end{pmatrix}. \tag{G15}
$$

Numerical evaluation is straightforward and fast, noting that we only require $j_i \lesssim 10$ because the perturbation theory kernels F_n and G_n involve only low-order Legendre polynomials.

---

[1] The Dark Energy Survey Collaboration, arXiv:astro-ph/0510346.

[2] K. S. Dawson, J.-P. Kneib, W. J. Percival, S. Alam, F. D. Albareti, S. F. Anderson, E. Armengaud, É. Aubourg, S. Bailey, J. E. Bautista et al., Astron. J. **151**, 44 (2016).

[3] M. Levi, C. Bebek, T. Beers, R. Blum, R. Cahn, D. Eisenstein, B. Flaugher, K. Honscheid, R. Kron, O. Lahav, P. McDonald, N. Roe, D. Schlegel, and representing the DESI collaboration, arXiv:1308.0847.

[4] R. Laureijs, J. Amiaux, S. Arduini, J. Auguères, J. Brinchmann, R. Cole, M. Cropper, C. Dabin, L. Duvet, A. Ealet et al., arXiv:1110.3193.

[5] D. Spergel, N. Gehrels, C. Baltay, D. Bennett, J. Breckinridge, M. Donahue, A. Dressler, B. S. Gaudi, T. Greene, O. Guyon, C. Hirata et al., arXiv:1503.03757.

[6] LSST Dark Energy Science Collaboration, arXiv:1211.0310.

[7] O. Doré, J. Bock, M. Ashby, P. Capak, A. Cooray, R. de Putter, T. Eifler, N. Flagey, Y. Gong, S. Habib et al., arXiv:1412.4872.

[8] M. H. Goroff, B. Grinstein, S. J. Rey, and M. B. Wise, Astrophys. J. **311**, 6 (1986).

[9] B. Jain and E. Bertschinger, Astrophys. J. **431**, 495 (1994).

[10] R. Scoccimarro and J. Frieman, Astrophys. J. Suppl. Ser. **105**, 37 (1996).

[11] R. Scoccimarro and J. A. Frieman, Astrophys. J. **473**, 620 (1996).

[12] D. Blas, M. Garny, and T. Konstandin, J. Cosmol. Astropart. Phys. 09 (2013) 024.

[13] Ya. B. Zeldovich, Astron. Astrophys. **5**, 84 (1970).

[14] F. R. Bouchet, S. Colombi, E. Hivon, and R. Juszkiewicz, Astron. Astrophys. **296**, 575 (1995).

[15] T. Matsubara, Phys. Rev. D **77**, 063530 (2008).

[16] F. Bernardeau, S. Colombi, E. Gaztañaga, and R. Scoccimarro, Phys. Rep. **367**, 1 (2002).

[17] M. Crocce and R. Scoccimarro, Phys. Rev. D **73**, 063519 (2006).

[18] M. Pietroni, J. Cosmol. Astropart. Phys. 10 (2008) 036.

[19] F. Bernardeau, M. Crocce, and R. Scoccimarro, Phys. Rev. D **78**, 103521 (2008).

[20] J. Lesgourgues, S. Matarrese, M. Pietroni, and A. Riotto, J. Cosmol. Astropart. Phys. 06 (2009) 017.

[21] A. Taruya, T. Nishimichi, and S. Saito, Phys. Rev. D **82**, 063522 (2010).

[22] D. Baumann, A. Nicolis, L. Senatore, and M. Zaldarriaga, J. Cosmol. Astropart. Phys. 07 (2012) 051.

[23] J. J. M. Carrasco, M. P. Hertzberg, and L. Senatore, J. High Energy Phys. 09 (2012) 82.

[24] M. Pietroni, G. Mangano, N. Saviano, and M. Viel, J. Cosmol. Astropart. Phys. 01 (2012) 019.

[25] F. Bernardeau, M. Crocce, and R. Scoccimarro, Phys. Rev. D **85**, 123519 (2012).

[26] M. Crocce, R. Scoccimarro, and F. Bernardeau, Mon. Not. R. Astron. Soc. **427**, 2537 (2012).

[27] E. Pajer and M. Zaldarriaga, J. Cosmol. Astropart. Phys. 08 (2013) 037.

[28] T. Matsubara, Phys. Rev. D **90**, 043537 (2014).

[29] J. J. M. Carrasco, S. Foreman, D. Green, and L. Senatore, J. Cosmol. Astropart. Phys. 07 (2014) 056.

[30] L. Mercolli and E. Pajer, J. Cosmol. Astropart. Phys. 03 (2014) 006.

[31] J. J. M. Carrasco, S. Foreman, D. Green, and L. Senatore, J. Cosmol. Astropart. Phys. 07 (2014) 057.

[32] S. M. Carroll, S. Leichenauer, and J. Pollack, Phys. Rev. D **90**, 023518 (2014).

[33] R. A. Porto, L. Senatore, and M. Zaldarriaga, J. Cosmol. Astropart. Phys. 05 (2014) 022.

[34] A. Manzotti, M. Peloso, M. Pietroni, M. Viel, and F. Villaescusa-Navarro, J. Cosmol. Astropart. Phys. 09 (2014) 047.

[35] L. Senatore and M. Zaldarriaga, J. Cosmol. Astropart. Phys. 02 (2015) 013.

[36] Z. Vlah, U. Seljak, and T. Baldauf, Phys. Rev. D **91**, 023508 (2015).

[37] U. Seljak and Z. Vlah, Phys. Rev. D **91**, 123516 (2015).

[38] Z. Vlah, M. White, and A. Aviles, J. Cosmol. Astropart. Phys. 09 (2015) 014.

[39] Z. Vlah, U. Seljak, M. Yat Chu, and Y. Feng, J. Cosmol. Astropart. Phys. 03 (2016) 057.

[40] M. McQuinn and M. White, J. Cosmol. Astropart. Phys. 01 (2016) 043.

[41] M. Schmittfull, Z. Vlah, and P. McDonald, Phys. Rev. D **93**, 103528 (2016).

[42] J. E. McEwen, X. Fang, C. M. Hirata, and J. A. Blazek, J. Cosmol. Astropart. Phys. 09 (2016) 015.

[43] N. McCullagh and A. S. Szalay, Astrophys. J. **752**, 21 (2012).

[44] B. D. Sherwin and M. Zaldarriaga, Phys. Rev. D **85**, 103523 (2012).

[45] J. R. Fergusson, D. M. Regan, and E. P. S. Shellard, Phys. Rev. D **86**, 063511 (2012).

[46] D. M. Regan, M. M. Schmittfull, E. P. S. Shellard, and J. R. Fergusson, Phys. Rev. D **86**, 123524 (2012).

[47] M. M. Schmittfull, D. M. Regan, and E. P. S. Shellard, Phys. Rev. D **88**, 063512 (2013).

[48] Z. Slepian and D. J. Eisenstein, Mon. Not. R. Astron. Soc. **448**, 9 (2015).

[49] M. Schmittfull, T. Baldauf, and U. Seljak, Phys. Rev. D **91**, 043530 (2015).

[50] Z. Slepian and D. J. Eisenstein, arXiv:1607.03109.

[51] E. Komatsu, D. N. Spergel, and B. D. Wandelt, Astrophys. J. **634**, 14 (2005).

[52] J. R. Fergusson, M. Liguori, and E. P. S. Shellard, Phys. Rev. D **82**, 023502 (2010).

[53] K. M. Smith, L. Senatore, and M. Zaldarriaga, arXiv: 1502.00635.

[54] V. Böhm, M. Schmittfull, and B. D. Sherwin, Phys. Rev. D **94**, 043519 (2016).

[55] A. Taruya, F. Bernardeau, T. Nishimichi, and S. Codis, Phys. Rev. D **86**, 103528 (2012).

[56] M. Cataneo, S. Foreman, and L. Senatore, arXiv: 1606.03633.

[57] D. Tseliakhovich and C. Hirata, Phys. Rev. D **82**, 083520 (2010).

[58] M. Fasiello and Z. Vlah, Phys. Rev. D **94**, 063516 (2016).

[59] A. Taruya, Phys. Rev. D **94**, 023504 (2016).

[60] The right-hand side of Eq. (18) follows by decomposing scalar products between wave vectors into spherical harmonics using Eq. (G3). Then angular integrals over $\hat{\mathbf{q}}_1$ and $\hat{\mathbf{q}}_2$ follow from orthogonality of Y_{lm}'s, and $\sum_{m'} Y_{\ell' m'}(\hat{\mathbf{k}}) Y^*_{\ell' m'}(\hat{\mathbf{k}}) = (2\ell' + 1)/(4\pi)$ gives Eq. (18).

[61] One way to derive the right-hand side of Eq. (21) proceeds as follows: Expand the Dirac delta in plane waves and each of those in spherical harmonics; decompose scalar products between wave vectors in spherical harmonics; integrate over $\hat{\mathbf{q}}_i$ and $\hat{\mathbf{r}}$ using Eq. (G4) and orthogonality of Y_{lm}'s; sum over m'_1 and m'_2 using Eq. (G8); use Eq. (G6) for $\sum_{\mathbf{L}} \mathcal{G}^{MM_2,-M_2}_{LL_2\tilde{L}_2} Y^*_{LM}(\hat{\mathbf{k}})$; use Eqs. (G9) and (G10).

[62] A. J. S. Hamilton, Mon. Not. R. Astron. Soc. **312**, 257 (2000).

[63] The right-hand side of Eq. (24) follows similarly to before: Expand the Dirac delta and scalar products between wave vectors in spherical harmonics, perform all angular integrations and sum over m's. One subtlety is that we averaged over orientations of the external $\mathbf{k}$. This does not affect the total physical power spectrum because we assume isotropy and ignored redshift space distortions (RSD). Even if individual contributions did depend on $\hat{\mathbf{k}}$ we could still integrate over $\hat{\mathbf{k}}$, because if $P = P_1 + P_2$ then $4\pi P = \int_{\hat{\mathbf{k}}} P = \int_{\hat{\mathbf{k}}} P_1 + \int_{\hat{\mathbf{k}}} P_2$. We note that RSD can be included in this framework by expressing the observable redshift space power spectrum in terms of isotropic statistics of the mass and velocity densities as discussed in Sec. VI F.

[64] To simplify the integral in Eq. (28) we introduce the auxiliary variable $\mathbf{q}_3 \equiv s_0\mathbf{k} + s_1\mathbf{q}_1 + s_2\mathbf{q}_2$ using a Dirac delta. The right-hand side then follows by decomposing scalar products into spherical harmonics, and expanding the Dirac delta in plane waves and those in spherical harmonics. Performing angular integrations over $\hat{\mathbf{q}}_i$, $\hat{\mathbf{r}}$ and $\hat{\mathbf{k}}$ using Eq. (G4) leads to a product of four Gaunt integrals, whose sum over m's is a Wigner 6-j symbol, giving Eq. (28). We also used Eq. (G13).

[65] This follows by introducing $\mathbf{q}_3 = \mathbf{q}_1 + \mathbf{q}_2$ with a Dirac delta, expanding this in spherical harmonics, performing all angular integrals, and using Eq. (G13).

[66] M. Peskin and D. Schroeder, *An Introduction to Quantum Field Theory, Advanced book classics* (Addison-Wesley Publishing Company, New York, 1995).

[67] The most general inverse Laplacian operator allowed by the arguments of the F_3 kernel in the 3-3 correlation (23) is $|s_1\mathbf{q}_1 + s_2\mathbf{q}_2 + s_3\mathbf{q}_3|^{-2}$ with $s_i \in \{0, 1\}$. We only consider a single inverse Laplacian in this section. The only case not already covered by Eq. (24) arises if two s_i are 1 and the other one is 0. Without loss of generality, we consider $(s_1, s_2, s_3) = (1, 1, 0)$, corresponding to $|\mathbf{q}_1 + \mathbf{q}_2|^{-2}$, or, slightly more generally, $|\mathbf{q}_1 + \mathbf{q}_2|^{-n_4}$.

[68] Z. Slepian and D. J. Eisenstein, Mon. Not. R. Astron. Soc. **454**, 4142 (2015).

[69] T. Hahn, Comput. Phys. Commun. **168**, 78 (2005).

[70] P. Catelan, Mon. Not. R. Astron. Soc. **276**, 115 (1995).

[71] P. Catelan and T. Theuns, Mon. Not. R. Astron. Soc. **282**, 455 (1996).

[72] C. Rampf and T. Buchert, J. Cosmol. Astropart. Phys. 06 (2012) 021.

[73] M. Schmittfull, Y. Feng, F. Beutler, B. Sherwin, and M. Y. Chu, Phys. Rev. D **92**, 123522 (2015).

[74] Z. Vlah, M. White, and A. Aviles, J. Cosmol. Astropart. Phys. 09 (2015) 014.

[75] R. Takahashi, Prog. Theor. Phys. **120**, 549 (2008).

[76] P. McDonald and A. Roy, J. Cosmol. Astropart. Phys. 08 (2009) 020.

[77] V. Desjacques, D. Jeong, and F. Schmidt (to be published).

[78] J. C. Jackson, Mon. Not. R. Astron. Soc. **156**, 1P (1972).

[79] N. Kaiser, Mon. Not. R. Astron. Soc. **227**, 1 (1987).

[80] A. J. S. Hamilton, Linear redshift distortions: A review, in *The Evolving Universe*, Astrophysics and Space Science Library Vol. 231, edited by D. Hamilton (Kluwer Academic Publishers, Dordrecht, 1998) p. 185.

[81] R. Scoccimarro, Phys. Rev. D **70**, 083007 (2004).

[82] D. Jeong and E. Komatsu, Astrophys. J. **651**, 619 (2006).

[83] A. Challinor and A. Lewis, Phys. Rev. D **84**, 043516 (2011).

[84] B. A. Reid and M. White, Mon. Not. R. Astron. Soc. **417**, 1913 (2011).

[85] U. Seljak and P. McDonald, J. Cosmol. Astropart. Phys. 11 (2011) 039.

[86] Z. Vlah, U. Seljak, P. McDonald, T. Okumura, and T. Baldauf, J. Cosmol. Astropart. Phys. 11 (2012) 009.

[87] Z. Vlah, U. Seljak, T. Okumura, and V. Desjacques, J. Cosmol. Astropart. Phys. 10 (2013) 053.

[88] T. Okumura, U. Seljak, P. McDonald, and V. Desjacques, J. Cosmol. Astropart. Phys. 02 (2012) 010.

[89] T. Okumura, U. Seljak, and V. Desjacques, J. Cosmol. Astropart. Phys. 11 (2012) 014.

[90] Note that some of the references use stronger approximations, dropping some terms compared to the DF approach. We are interested here in comparing the PT structure (especially angular) of these results where they overlap, disregarding the differences.

[91] T. Okumura, U. Seljak, Z. Vlah, and V. Desjacques, J. Cosmol. Astropart. Phys. 05 (2014) 003.

[92] J. Carlson, B. Reid, and M. White, Mon. Not. R. Astron. Soc. **429**, 1674 (2013).

[93] Z. Vlah, E. Castorina, and M. White, arXiv:1609.02908.

[94] In general, α coefficients enforce $\ell'_i \leq \ell_i$, where ℓ_i denote exponents of scalar products in the integrand of Eq. (24), and the 6-j symbol enforces four triangle conditions, restricting $|\ell'_2 - \ell'_3| \leq L_1 \leq \ell'_2 + \ell'_3$, and similarly for L_2 and L_3, as well as $|L_2 - L_3| \leq L_1 \leq L_2 + L_3$. Additionally, the modified 6-j symbol (G14) enforces $L_1 + L_2 + L_3$, $L_1 + \ell'_2 + \ell'_3$, $L_2 + \ell'_1 + \ell'_3$ and $L_3 + \ell'_1 + \ell'_2$ to be even. The coupling factor has the same symmetry properties as the 6-j symbol.

[95] Similarly to the calculation in Appendix D, angular integrations lead to four Gaunt integrals. Due to slightly different couplings the sum over m's yields a 6-j symbol, leading to the coupling factor $\mathcal{M}_3$.

[96] "NIST Digital Library of Mathematical Functions," http://dlmf.nist.gov/, Release 1.0.5 of 2012-10-01, online companion to [97].

[97] F. W. J. Olver, D. W. Lozier, R. F. Boisvert, and C. W. Clark, eds., *NIST Handbook of Mathematical Functions* (Cambridge University Press, Cambridge, England, 2010) print companion to [96].

[98] G. N. Watson, *A Treatise on the Theory of Bessel Functions* (Cambridge University Press, Cambridge, England, 1966).